Journal of Inflammation Research

Dovepress
Taylor & Francis Group

Open Access Full Text Article

ORIGINAL RESEARCH

Combined Analysis of Transcriptome and Mendelian Randomization Reveals *AKT1* and *PPARG* as Biomarkers Related to Glucose Metabolism in Sepsis

Jie Ma[1,2,*], Wendi Li[3], Qianqian Ma[1], Liying Ding[4], Zhaoyun Wang[1], Rong Wang[1], Yanan Huang[1], Gang Ma[2,*], Jun Gao[1,*]

[1]Department of Anesthesia and Perioperative Medicine, First People's Hospital of Yinchuan, The Second Clinical Medical College of Ningxia Medical University, Yinchuan, Ningxia, 750001, People's Republic of China; [2]Department of Anesthesia and Perioperative Medicine, General Hospital of Ningxia Medical University, The First Clinical Medical College of Ningxia Medical University, Yinchuan, Ningxia, 750004, People's Republic of China; [3]Department of Child Rehabilitation Education, Ningxia Rehabilitation Center for the Disabled, Yinchuan, Ningxia, 750002, People's Republic of China; [4]Department of Gynecology, Gynecology Clinic of Li Ying, Wuzhong, Ningxia, 751100, People's Republic of China

*These authors contributed equally to this work

Correspondence: Gang Ma, Department of Anesthesia and Perioperative Medicine, General Hospital of Ningxia Medical University, The First Clinical Medical College of Ningxia Medical University, Yinchuan, Ningxia, 750004, People's Republic of China, Email magang2671@163.com; Jun Gao, Department of Anesthesia and Perioperative Medicine, First People's Hospital of Yinchuan, The Second Clinical Medical College of Ningxia Medical University, Yinchuan, Ningxia, 750001, People's Republic of China, Email gaojun1605@sina.com

Introduction: This study aimed to identify diagnostic and therapeutic biomarkers related to glucose metabolism in sepsis, as hyperglycemia and blood glucose fluctuations influence sepsis progression.

Methods: Datasets from public databases were analyzed using various methods, including differential expression analysis, PPI network screening, machine learning algorithms and Mendelian randomization. A nomogram model was developed, and biomarker functions were explored through enrichment analysis, immunoinfiltration analysis, transcription factors (TFs) and microRNA (miRNA) prediction, and drug prediction. Quantitative reverse transcription-polymerase chain reaction (qRT-PCR) was performed to validate the expression of biomarkers in sepsis and control group.

Results: There were 3,899 differential expressed genes (DEGs) in sepsis, with 141 related to glucose metabolism. Eleven hub genes were identified from the PPI network, and six biomarkers were selected through machine learning and area under the curve (AUC) validation. Notably, *PPARG* (OR = 1.0730, 95% CI: 1.0330–1.1160) and *AKT1* (OR = 0.9211, 95% CI: 0.8569–0.9902) had causal relationships with sepsis. The diagnostic nomogram based on these biomarkers showed good efficacy. Enrichment analysis suggested *AKT1* inhibits sepsis development, while *PPARG* promotes it. Drug prediction indicated strong interactions between *AKT1* and gigantol, and *PPARG* with echinatin. qRT-PCR showed reduced expression of *PPARG* and *AKT1* in sepsis, aligning with bioinformatics predictions.

Conclusion: In summary, *AKT1* and *PPARG* are causally associated with sepsis, showing diagnostic potential. *AKT1* may inhibit sepsis development, while *PPARG* may promote it. These findings provide valuable insights for sepsis diagnosis and therapeutic drug development.

Keywords: sepsis, glucose metabolism, transcriptomics, Mendelian randomization, biomarkers

Introduction

Sepsis is a dysregulation of the host's systemic inflammatory and immune responses to infection, leading to life-threatening organ dysfunction.[1] It is a common complication following serious infections, trauma, burns, shock and major surgery, characterised by a high prevalence, severity, mortality and health care costs.[2,3] A global observational study in 2017 showed that approximately 10 million patients died due to sepsis, accounting for approximately 20% of the total mortality in that year.[4,5] In addition, sepsis patients accounted for the majority of admissions to intensive care units,

Received: 8 April 2025
Accepted: 12 July 2025
Published: 30 July 2025

with a 90-day mortality rate of 35.5%, according to a 2020 study conducted in mainland China.[6] In addition to causing serious damage to patients' health, sepsis also imposes a heavy economic burden on the healthcare sector, reportedly amounting to US$24 billion per year worldwide.[7] The World Health Organization has described sepsis as a serious global public health problem and designated it as a "global health priority" in 2017. Currently, despite advances in clinical care and research methods, sepsis is a heterogeneous syndrome characterised by a wide range of clinical and biological features, which has hindered the development and advancement of the field of sepsis care.[8] It has been suggested that deeper and broader research into altering signalling pathways, gene targeting to modify the characteristically high and or low immune response, prevention by optimising the microbiome and the molecular pathways of the immune response in sepsis may improve the prognosis of sepsis.[9] Conventional biomarkers such as CRP, PCT and cytokines are not sensitive and specific enough to be used exclusively for patient diagnosis and prognosis.[10] Therefore, further research into the pathogenesis and treatment of sepsis is of great theoretical importance and clinical value. It is imperative that we find sensitive and specific biomarkers as early as possible to aid in the early diagnosis, prognosis and treatment of sepsis.

Glucose is the primary energy source in animals and an important precursor for the synthesis of nucleic acids, lipids, and other macromolecules. Infections can affect the absorption, transport, and metabolism of glucose by cells.[11] During sepsis, various degrees of glucose metabolism disorders are commonly observed.[12] Glucose metabolism includes aerobic oxidation and glycolysis. In aerobic oxidation, one molecule of glucose is completely oxidized to produce 36 (or 38) molecules of ATP, which serves as the main energy source in the body. Under anaerobic conditions, glucose is converted to lactic acid through glycolysis, yielding only 2 molecules of ATP.[13] Recent studies have shown that in the cytoplasm, glucose is broken down into two pyruvate molecules via glycolysis before entering the mitochondria. Within the mitochondria, a large amount of ATP and water is generated through the tricarboxylic acid cycle and oxidative phosphorylation, releasing carbon dioxide. However, during sepsis, cells may experience mitochondrial dysfunction due to inflammation and oxidative stress, leading to a reliance on glycolysis to meet energy demands even in the presence of sufficient oxygen. This results in excessive production and abnormal accumulation of lactic acid.[14] Sepsis patients exhibit suppressed glucose oxidation while increasing fatty acid oxidation. Preclinical studies have indicated that glucose metabolism is detrimental in bacterial sepsis, while fasting metabolism appears to be protective.[12] Furthermore, studies have found that NORAD and nuclear proteins play important roles in regulating glucose metabolism and immune responses under septic conditions.[15,16] These findings underscore the significance of glucose metabolism in the context of sepsis. Further research is needed to explore new therapeutic strategies targeting glucose metabolism to improve outcomes for sepsis patients.

Mendelian randomization (MR) is a method used to infer causal relationships between exposure and outcome.[17] This study utilized transcriptomic techniques and Mendelian randomization analysis to explore biomarkers related to glucose metabolism that have a causal relationship with sepsis. Additionally, the study employed immune infiltration drug prediction methods to further investigate the potential functions of these biomarkers. Overall, this research conducted an in-depth analysis of glucose metabolism-related genes and their functional characteristics in sepsis through a series of bioinformatics techniques, aiming to identify novel diagnostic targets for sepsis and provide a theoretical basis for personalized treatment of the condition.

Material and Methods

Data Source

The expression profiling datasets GSE65682 and GSE134347 of sepsis were downloaded from the Gene Expression Omnibus (GEO) database (https://www.ncbi.nlm.nih.gov/geo/). Dataset GSE65682 served as the training set for this study, including 479 sepsis samples and 42 control samples. Dataset GSE134347 was used as the validation set, containing 156 sepsis samples and 82 control samples. Glucose metabolism-related genes (GMRGs)[18] were retrieved from previous study, and detailed gene information was provided in Table S1.

Identification and Analysis of Differentially Expressed Glucose Metabolism Related Genes (DE-GMRGs) in Sepsis

Differentially expressed genes (DEGs) between sepsis and control samples were identified using the limma package (v 3.54.0),[19] with differential screening conditions set at $\log_2$FoldChange (FC) < 0.5 and P.value < 0.05. The expression of DEGs was

visualized using ggplot2 (v 3.4.1)[20] and pheatmap.[21] The DE-GMRGs were then identified by taking the intersection of the DEGs and the GMRGs using the ggvenn package (v 1.7.1).[22]

Enrichment Analysis of DE-GMRGs and Construction of Protein-Protein Interaction (PPI) Network

DE-GMRGs were analyzed using Gene Ontology (GO) and the Kyoto Encyclopedia of Genes and Genomes (KEGG) with the clusterProfiler package (v 4.7.1.001)[23] ($P < 0.05$) for a preliminary exploration of their biological functions. The GO enrichment analysis included biological processes (BP), cellular components (CC), and molecular functions (MF). The treemap package (v 3.4–3)[24] was used to visualize the top 10 most significant entries in each GO category and to highlight the major enrichment pathways in KEGG. Additionally, the disease ontology (DO) function of DE-GMRGs was studied using the WebGestalt online database. The protein-level interactions among DE-GMRGs were established through STRING (https://string-db.org/) with a low confidence threshold of 0.4, and the PPI network was visualized using Cytoscape (v 3.7.2).[25] DE-GMRGs were then filtered through the Degree, Bottleneck, and Betweenness algorithms in the cytoHubba, with hub genes identified from the intersection of genes filtered by these algorithms for further analysis.

Screening and Validation of Diagnostic Efficacy of Biomarkers

The hub gene was further screened using machine learning algorithms. Three machine learning algorithms included support vector machine-recursive feature elimination (SVM-RFE) analysis based on the e1071 package (v 1.7–12),[26] least absolute shrinkage and selection operator (LASSO) algorithm based on the glmnet package (v 4.1.8),[27] and Boruta analysis using the Boruta package (v 8.0.0).[28] The genes selected by machine learning methods were intersected, and the resulting genes were designated as potential biomarkers. Subsequently, we analyzed the differences in expression levels of potential biomarkers in the training and validation sets using the Wilcoxon test. To evaluate the diagnostic capability of these potential biomarkers, we generated receiver operating characteristic (ROC) curves and calculated the area under the curve (AUC) using the pROC package (v 1.18.5)[29] in the training set and the validation sets. Potential biomarkers passing through the validation were defined as biomarkers of sepsis.

MR Analysis

To investigate the causal relationship between the biomarkers and sepsis, we conducted MR analysis, using the biomarkers as the exposure variable and sepsis as the outcome variable. Expression quantitative trait loci (eQTL) data for the biomarkers were sourced from the Integrative Epidemiology Unit (IEU) Open Genome-Wide Association Study (GWAS) database (https://gwas.mrcieu.ac.uk/). Summary phenotypic data for sepsis (eu-b-4980) were obtained from the UK Biobank (https://gwas.mrcieu.ac.uk/) database, which included 12,243,539 single nucleotide polymorphisms (SNPs) from 486,484 Europeans (11,643 sepsis samples and 474,841 controls). The MR analysis was based on those key assumptions: (1) a robust and significant association between instrumental variables (IVs) and sepsis; (2) no causal relationship between IVs and other confounders; and (3) IVs affect sepsis only through the biomarkers.

To enhance the accuracy of the MR analysis, we utilized the TwoSampleMR package (v 0.5.6)[30] to rigorously control the selection of IVs. The following steps were implemented: (1) SNPs significantly associated with the biomarker eQTL were selected using a threshold of $P < 5 \times 10^{-5}$; (2) SNPs in linkage disequilibrium (LD) were removed, with parameters set as $r^2 = 0.1$ and kb = 10; (3) The statistical value (F) of the IVs was calculated using the formula: $F = \frac{(N-k-1)}{k} \times \frac{R}{1-R^2}$, where N represented the number of sepsis samples in GWAS, k was the number of IVs, and R^2 was the variance proportion of IVs explaining the biomarker eQTL. The harmonise_data function was employed to unify effect alleles and effect sizes, sepsis related IVs were excluded to ensure consistency across datasets. For the MR analysis, we applied 5 methods, including MR Egger,[31] weighted median,[32] inverse variance weighted (IVW),[33] simple mode,[30] and weighted mode.[34] IVW was used as the primary method to identify genes with a significant causal relationship with sepsis as biomarkers ($P < 0.05$). Finally, sensitivity analyses were conducted to assess the robustness of the MR analyses, incorporating heterogeneity test,[35] horizontal pleiotropy test,[36] and the Leave-One-Out (LOO) test.[37]

Enrichment Analysis of Biomarkers

To further investigate the underlying mechanisms of sepsis, we analyzed the differences in biological processes associated with biomarkers that exhibit a causal relationship to the disease, comparing the sepsis to the control simple. We utilized the pathway enrichment file "c2.cp.kegg.v7.4.symbols.gmt" from the Gene Set Enrichment Analysis (GSEA) website (http://www.gsea-msigdb.org/gsea/msigdb) for enrichment analysis. In the training set, GSEA pathway enrichment analysis was conducted using the clusterProfiler package, focusing on the correlation between each biomarker and all genes, applying the criteria $|NES| > 1$ and $P < 0.05$.

Construction of the Nomogram for Sepsis

In order to comprehensively evaluate the diagnostic efficacy of biomarkers, we developed a nomogram using the rms package (v 6.8.2),[29] based on the expression levels of the biomarkers. We also established a calibration curve to assess the predictive accuracy of the nomogram. Additionally, we employed ROC analysis and decision curve analysis (DCA) to quantify the overall diagnostic performance of the model.

Immunoinfiltration Analysis

To assess the composition of the immune microenvironment in sepsis patients, we calculated the abundance of 28 types of immune cells in sepsis and control samples using ssGSEA of GSVA package (v 1.42.0)[38] based on the training set. Differences in immune cell infiltration between the two groups were analyzed using the Wilcoxon test. Subsequent analyses explored the correlation between biomarkers and immune cells with varying levels of infiltration across groups. The results were visualized using the ggplot2 package.

Transcription Factors (TFs) and microRNAs (miRNAs) Prediction of Biomarkers

In order to gain a deeper understanding of the interactions in biomarker regulatory networks, TFs of biomarkers were predicted using the ChEA3 database. The miRNAs related to these genes (target score > 50) were forecasted through the miRDB database (https://mirdb.org/mirdb/index.html). The regulatory network was visualized using Cytoscape.

Drug Prediction and Molecular Docking

To identify potential clinical drugs for sepsis, this study utilized the DGIdb database for drug prediction based on biomarkers (https://www.dgidb.org/) and visualized the network using Cytoscape software. Molecular docking was subsequently performed to analyze the interactions between biomarkers and their corresponding active components. The 3D structures of the biomarker proteins (in PDB format) were obtained from the Protein Data Bank, while the active components' 3D structures (in SDF format) were sourced from the PubChem database. For better analysis, the SDF files of the active ingredients were converted to PDB format using Babel GUI (v 3.1.1). PyMOL (v 3.1.1)[39] was employed to remove water molecules and small molecule ligands before conducting molecular docking with AutoDock Vina,[40] and the results were visualized using PyMOL (v 3.1.1).[39]

Clinical Samples

According to the predefined inclusion criteria, four cases of sepsis and four normal control samples were collected from the Second Affiliated Hospital of Ningxia Medical University (First People's Hospital of Yinchuan). The inclusion criteria were as follows: (1) Age between 18 and 75 years; (2) Blood samples; (3) Patients with a confirmed initial diagnosis of sepsis and healthy donors. Sepsis patients should meet the Sepsis-3.0 diagnostic criteria, have definite or highly suspected infections, and have a sequential organ failure score of ≥2. The exclusion criteria for the sepsis samples included the presence of severe comorbidities, such as advanced cardiac insufficiency, advanced liver insufficiency, and advanced renal insufficiency, as well as any documented immune deficiencies or autoimmune diseases. All patients and healthy donors or their legal representatives agreed to participate in the study and signed an informed consent form. This study was approved by the Ethics Committee of the Second Affiliated Hospital of Ningxia Medical University (First People's Hospital of Yinchuan) (No: KY-2025-175).

Construction of the Mouse Model

This study was performed in line with the principles of the Declaration of Helsinki and approved by the Institutional Animal Care and Use Committee of the Second Clinical Medical College of Ningxia Medical University (First People's Hospital of Yinchuan) (No: KY-2025-039). Male 8-wk-old mice on *C57BL/6J* background were purchased from Vital River Laboratory Animal Technology Co., Ltd (Beijing, China), which were feed in the Experimental Animal Center of Ningxia Medical University. All sepsis-induced mice were subjected to classic cecal ligation and puncture (CLP) to induce sepsis.[41] Briefly, for the sepsis group, mice were anesthetized with 2% isoflurane inhalation and placed on a heating pad to maintain a body temperature of 36–37 °C. After disinfecting the skin, a 1 cm incision was made along the abdominal midline approximately 1 cm below the genital area to expose the cecum. The cecum was ligated with 3–0 silk thread about 1 cm from its distal end. Using a 21G needle, two punctures were made at the tip of the ligated cecum, and a small amount of feces was extruded. Care was taken to avoid injuring blood vessels. The cecum was then carefully returned to the abdominal cavity, and the abdominal wall and skin were closed with interrupted sutures using 4–0 silk thread. The incision was infiltrated with 0.2% ropivacaine. Post-surgery, mice received 50 mL/kg of sterile saline pre-warmed to 37°C for fluid resuscitation. For the control group, the same procedure was followed for abdominal incision and cecum exposure, but without ligation or puncture. The duration of the procedures for both groups was consistent. All surgical procedures were performed by the same individual. At 24 hours postoperatively, blood was collected via cardiac puncture under 2% isoflurane anesthesia. Immediately following blood collection, the mice were euthanized by cervical dislocation. Randomized double blind study was employed.

Quantitative Reverse Transcription-Polymerase Chain Reaction (qRT-PCR)

Blood samples were collected from mice under septic and control conditions for qRT-PCR.[42] Total RNA was extracted using RNAeasy™ Blood RNA Isolation Kit with Spin Column (R0091M, Beyotime Biotechnology, China), and its concentration and purity were measured using a Nanodrop 2000 spectrophotometer. Total RNA was reverse-transcribed into cDNA with a reaction mixture containing 4 μL of 5×SweScript All-in-One SuperMix for qPCR (G3337, Servicebio, China), 1 μL gDNA Remover, 10 μL total RNA, and nuclease-free water to a final volume of 20 μL. Then, qRT-PCR was performed on the 2×Universal Blue SYBR Green qPCR Master Mix (G3326, Servicebio, China) to assess the mRNA expression of biomarkers. *GAPDH* was used as the internal reference gene, with primer sequences of biomarkers listed in Table 1. Relative mRNA expression levels were calculated using the $2^{-\Delta\Delta Ct}$ method. All assays were conducted in triplicate with biological replicates.

For clinical samples, blood samples were collected from clinical samples and control conditions. Total RNA extraction, quantification, and cDNA synthesis were performed identically to the mouse samples (as described above). Then, qRT-PCR was performed on the ArtiCan^{ATM} SYBR qPCR Mix (TSE501, Tsingke, China) to assess the mRNA expression of biomarkers. *Hs-ACTB* was used as the internal reference gene, with primer sequences of biomarkers listed in Table 2. Relative mRNA expression levels were calculated using the $2^{-\Delta\Delta Ct}$ method. All assays were conducted in triplicate with biological replicates.

Table 1 The Primer Sequences of Biomarkers in qRT-PCR

Gene	Primer Sequences
GAPDH	5′-CCTCGTCCCGTAGACAAAATG-3′ forward
	5′-TGAGGTCAATGAAGGGGTCGT-3′ reverse
AKT1	5′-TCAGGATGTGGATCAGCGAGAGTC-3′ forward
	5′-AGGCAGCGGATGATAAAGGTGTTG-3′ reverse
PPARG	5′-GCCAAGGTGCTCCAGAAGATGAC-3′ forward
	5′-GGTGAAGGCTCATGTCTGTCTCTG-3′ reverse

https://doi.org/10.2147/JIR.S528347

Table 2 The Primer Sequences of Biomarkers in qRT-PCR

Gene	Primer Sequences
Hs-ACTB	5′-CCTGGCACCCAGCACAAT-3′ forward
	5′-GGGCCGGACTCGTCATAC-3′ reverse
AKT1	5′-CTGTCATCGAACGCACCTTCC-3′ forward
	5′-AGTCCATCTCCTCCTCCTCCTG-3′ reverse
PPARG	5′-CCACATTACGAAGACATTCCATTCAC-3′ forward
	5′-AGATGCAGGCTCCACTTTGATTG-3′ reverse

Statistical Analysis

All analyses were conducted in R version 4.2.2. The Wilcoxon test was employed to compare differences between the two groups of samples during significance analysis of various parameters (such as expression levels and different eigenvalues). In the graphical representations, ns means have not significant difference, * means $P < 0.05$, ** means $P < 0.01$, *** means $P < 0.001$, **** means $P < 0.0001$.

Results

Function of DEGs and Screening of Hub Genes in Sepsis

Differential expression analysis based on the training set revealed 3,899 DEGs between sepsis and control samples, with 1,268 genes being highly expressed in sepsis samples and 2,631 genes being lowly expressed in sepsis samples (Figure 1A and 1B). The intersection of the DEGs and the GMRGs resulted in 141 DE-GMRGs (Figure 1C). Subsequently, the study analyzed the molecular functions and mechanisms of action associated with the DE-GMRGs. GO enrichment analysis indicated that DE-GMRGs were significantly enriched in 864 BP entries, 46 CC entries, and 90 MF entries, primarily involving metabolic processes such as monosaccharide metabolism, hexose metabolism, and glucose metabolism (Figure 1D). KEGG analysis showed that these DE-GMRGs were mainly involved in 82 metabolic and signal transduction pathways, including glycolysis/gluconeogenesis, carbon metabolism, and central carbon metabolism in cancer (Figure 1E). DO analysis also indicated that DE-GMRGs were primarily associated with blood diseases such as hemolysis disorder, myeloid leukemia, and hemoglobin adverse events (Figure 1F). These enrichment results suggest a correlation between the functions of DE-GMRGs and glucose metabolism in sepsis. The PPI network constructed from the DEGs contained 126 nodes and 827 edges, including *GAPDH*, *PGK1*, and *LDHA*, which were proteins with regulatory effects on sepsis (Figure 1G). Through the intersection of the top 20 genes identified using the Degree, Bottleneck, and Betweenness algorithms, we identified 11 hub genes for further analysis (Figure 1H).

Screening and Validation of 6 Biomarkers Related to Glucose Metabolism in Sepsis

Machine learning algorithms were employed to further screen the 11 hub genes identified in the training set. The LASSO algorithm selected 9 genes (Lambda.min = 0.0012) (Figure 2A), while the SVM-RFE algorithm identified 8 genes (Figure 2B). Boruta analysis yielded a total of 11 genes (Figure 2C). The intersection of the genes obtained from these machine learning approaches resulted in 6 potential biomarkers: *GAPDH*, *AKT1*, *TXN*, *DLAT*, *PPARG*, and *PGK1* (Figure 2D). The expression levels and diagnostic efficacy of these potential biomarkers were validated in both the training and validation sets. Boxplots demonstrated notable variations in the expression of these 6 genes between sepsis and control samples in both datasets, among them, the expression levels of *AKT1* and *DLAT* were decreased in sepsis samples, while *GAPDH*, *PGK1*, *PPARG* and *TXN* were significantly higher in sepsis samples (Figure 2E). ROC curve analysis revealed that the AUC values for *GAPDH* (0.94), *AKT1* (0.87), *TXN* (0.98), *DLAT* (0.91), *PPARG* (0.94), and *PGK1* (0.84) in the training set confirmed their diagnostic efficacy for sepsis. In the validation set, the AUC values for these biomarkers were also promising: *GAPDH* (0.88), *AKT1* (0.90), *TXN* (1.00), *DLAT* (0.89), *PPARG* (0.98), and *PGK1* (0.93), indicating their potential as reliable biomarkers for sepsis (Figure 2F).

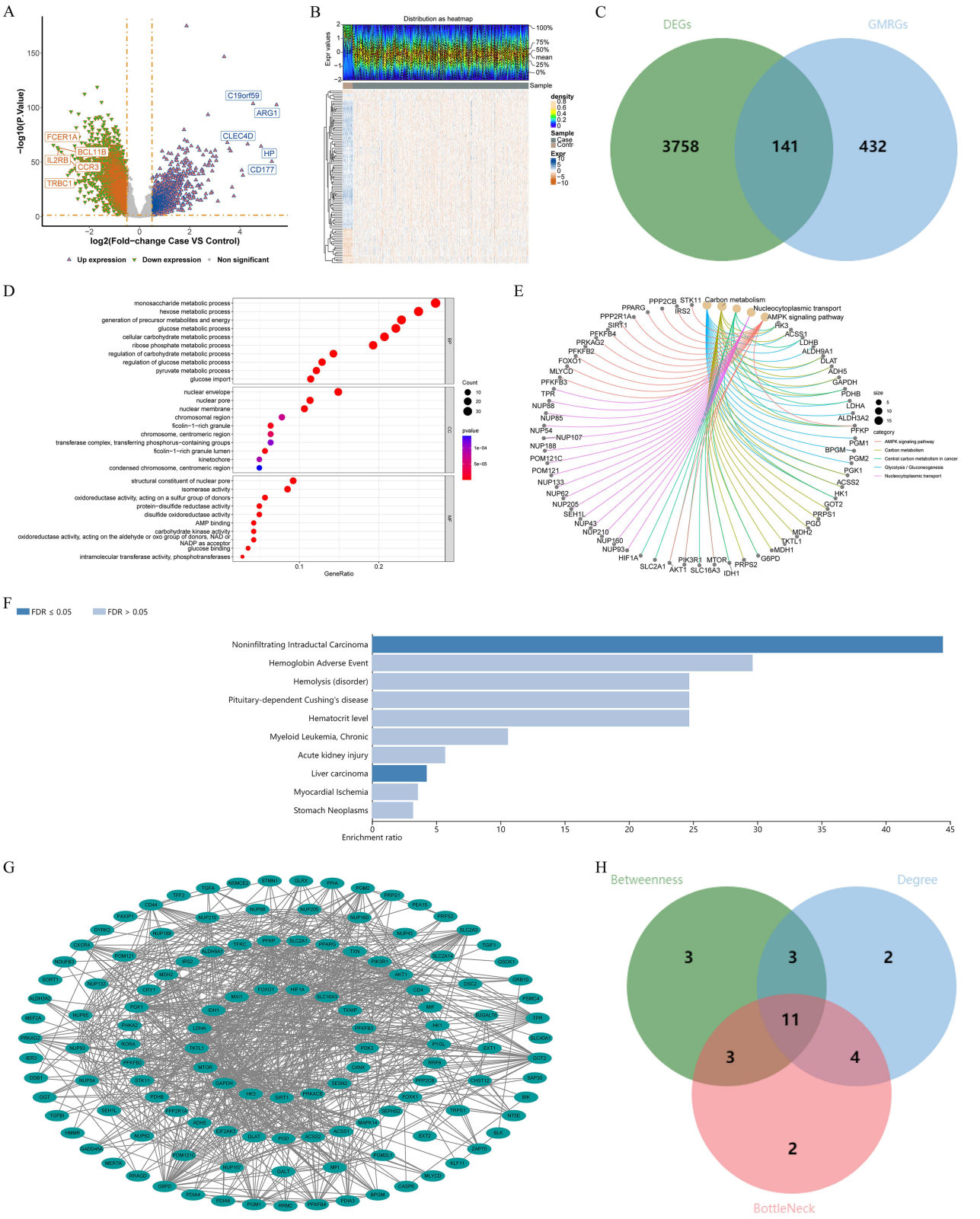

Figure 1 Identification of differentially expressed genes (DEGs) and hub genes in sepsis. (**A**) The volcano map of DEGs. The blue equilateral triangle represents up-regulated DEGs, the green inverted triangle represents down-regulated DEGs, and the gray represents genes that are not statistically significant; (**B**) The heatmap of DEGs. The abscissa represents samples, the ordinate represents genes, blue is high expression gene, yellow is low expression gene; (**C**) Identification of the differentially expressed glucose metabolism-related genes (DE-GMRGs) in sepsis; (**D**) Gene ontology (GO) functional enrichment analysis of DE-GMRGs; (**E**) Kyoto encyclopedia of genes and genomes (KEGG) enrichment analysis of DE-GMRGs; (**F**) Disease ontology (DO) enrichment analysis of DE-GMEGs; (**G**) The protein-protein interaction (PPI) network of DE-GMEGs; (**H**) The venn diagram of hub gene.

https://doi.org/10.2147/JIR.S528347

Significant Causal Relationship Between *PPARG*, *AKT1* and Sepsis

To explore the causal relationship between 6 biomarkers and sepsis, a MR analysis was conducted, treating the biomarkers as exposure variables and sepsis as the outcome variable. *PGK1* was excluded due to the absence of eQTL data. For the remaining 5 biomarkers, 556 SNPs with F values greater than 10 were identified, confirming their strength as IVs suitable for MR analysis (Table S2). Subsequent steps involved aligning the effect allele with the effect size, resulting in a total of 533 SNPs after excluding those significantly associated with sepsis. The MR analysis revealed significant associations between sepsis and *GAPDH*, *PPARG*, *TXN*, and *AKT1* ($P < 0.05$ for the IVW algorithm). Notably, *PPARG* [odds ratio (OR) = 1.0730, 95% confidence interval (CI): 1.0330–1.1160] and *TXN* [OR = 1.0726, 95% CI: 1.0084–1.1409] were identified as risk factors for the development of sepsis. Conversely, *GAPDH* [OR = 0.9100, 95% CI: 0.8670–0.9550] and *AKT1* [OR = 0.9211, 95% CI: 0.8569–0.9902] were found to be protective factors against sepsis (Table 3). The correlation trends between the biomarkers and sepsis were illustrated in scatter plots (Figure 3A and B, Figure S1A and B), indicating that higher expression of *PPARG* and *TXN* was associated with an increased risk of sepsis, whereas higher expression of *AKT1*

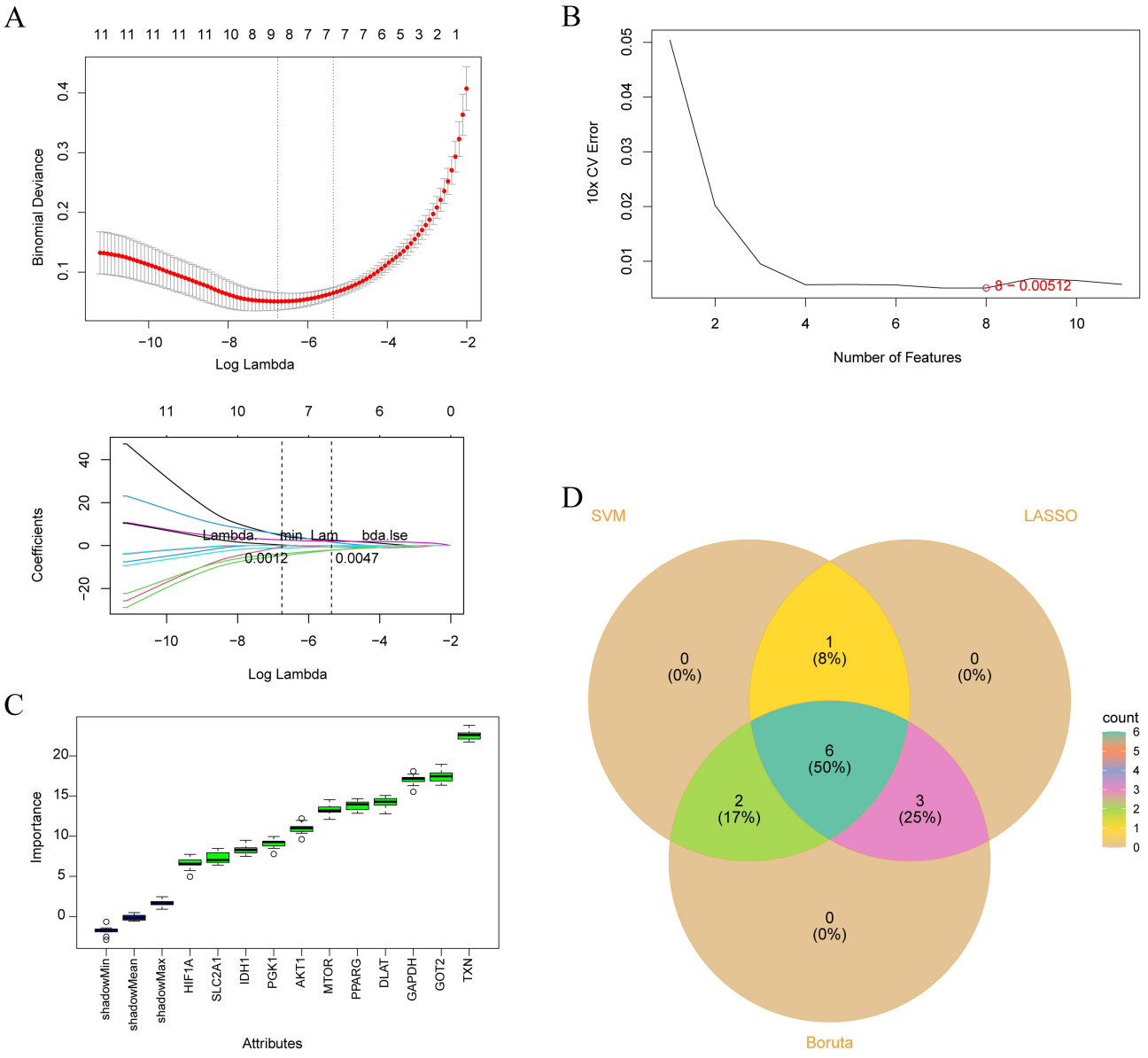

Figure 2 Continued.

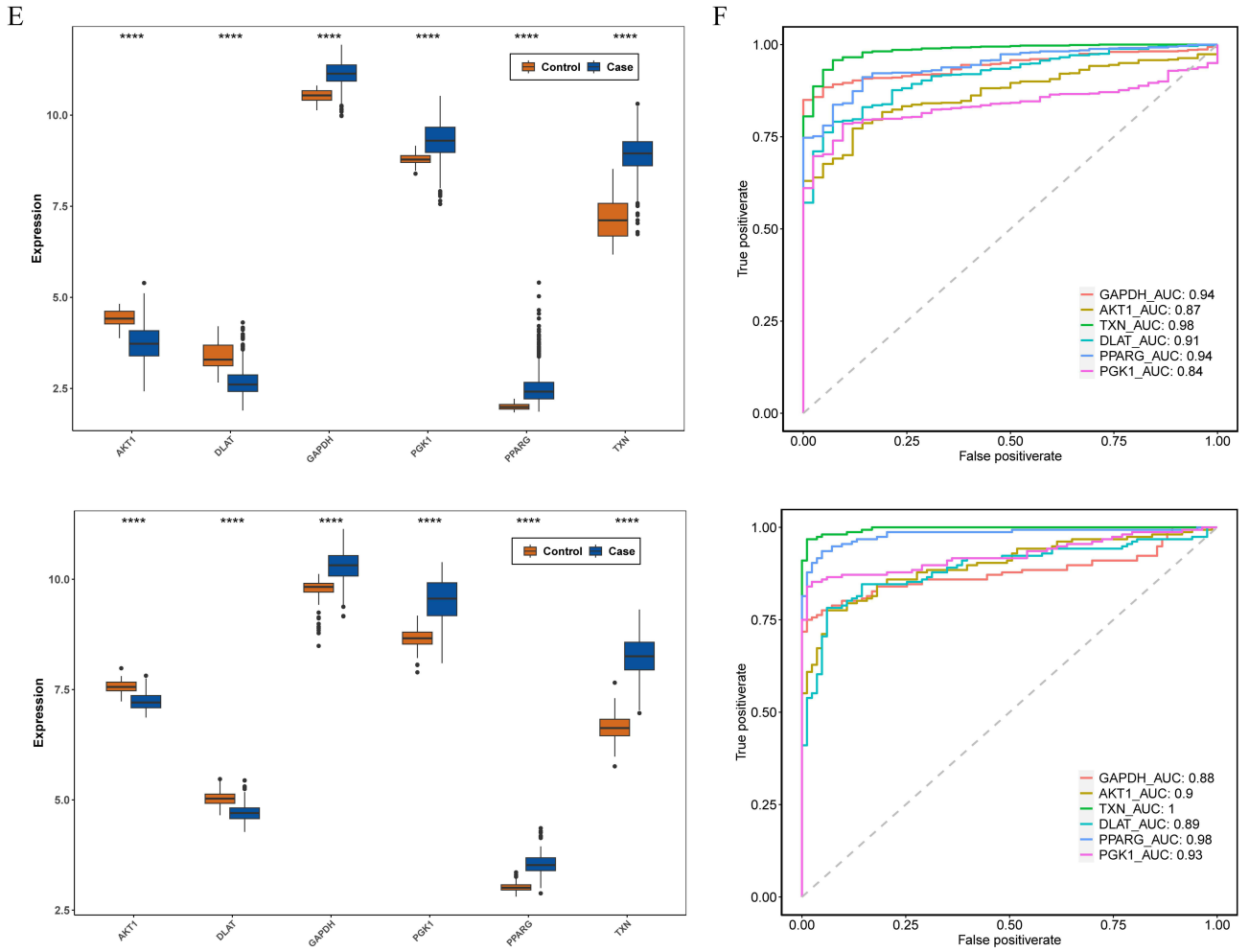

Figure 2 Screening and verification of 6 biomarkers in sepsis. (**A**) The least absolute shrinkage and selection operator (LASSO) regression analysis of the DE-GMRGs; (**B**) The support vector machine-recursive feature elimination (SVM-RFE) analysis of the DE-GMRGs; (**C**) The Boruta analysis of the DE-GMRGs; (**D**) The Venn diagram of potential biomarkers; (**E**) Expression of potential biomarkers in sepsis and control samples. The left graph represents the training set, the right figure represents the verification set; (**F**) The receiver operating characteristic (ROC) curve of the potential biomarkers in the training and validation sets. AUC, area under the curve.

and *GAPDH* might reduce the risk of sepsis. The efficacy of each SNP locus in assessing biomarkers for sepsis diagnosis was presented in forest plots (Figure 3C and D, Figure S1C and D). The distribution of SNPs screened in this study aligns with Mendel's second law, demonstrating a relatively even distribution and reinforcing the credibility of the findings (Figure 3E and F, Figure S1E and F).

To further validate the robustness of the findings, the sensitivity analysis was performed. Cochran's Q test indicated no heterogeneity in MR analysis ($P > 0.05$) (Table S3). Additionally, the horizontal pleiotropy test revealed no evidence of confounding bias for all genes except *TXN* ($P > 0.05$) (Table S4). The LOO of SNPs further confirmed the reliability of the study results (Figure 3G and H, Figure S1G and H). Combining the MR analysis with transcriptomic data, the expression patterns of *PPARG* and *AKT1* were consistent with the identified trends. Consequently, these 2 genes were recognized as biomarkers with a causal relationship to sepsis, warranting further investigation.

Nomogram Based on *PPARG* and *AKT1* with Reliable Diagnostic Capability

After identifying *PPARG* and *AKT1* as biomarkers causally associated with sepsis, GSEA was conducted to explore their biological functions. *PPARG* was found to enrich 52 pathways, primarily associated with the inhibition of pathways such as "ribosome", "graft versus host disease", "type I diabetes mellitus" and "cell adhesion molecules" (Figure 4A). In contrast, *AKT1*

https://doi.org/10.2147/JIR.S528347

Table 3 Mendelian randomization analysis results of biomarker and sepsis

Id.Exposure	Id.Outcome	Outcome	Exposure	Method	nsnp	b	se	pval	lo_ci	up_ci	or	or_lci95	or_uci95	pleio_P	heter_P
eqtl-a-ENSG00000111640(*GAPDH*)	ieu-b-5086	Sepsis	|| id:eqtl-a-ENSG00000111640	MR Egger	84	-0.1266	0.0410	0.0027	-0.2069	-0.0463	0.8810	0.8130	0.9550	0.3211	0.4400
				Weighted median		-0.0954	0.0352	0.0067	-0.1644	-0.0265	0.9090	0.8480	0.9740	0.3211	0.4400
				Inverse variance weighted (fixed effects)		-0.0942	0.0247	0.0001	-0.1426	-0.0457	0.9100	0.8670	0.9550	0.3210	0.4400
				Simple mode		-0.0995	0.0533	0.0652	-0.2039	0.0049	0.9050	0.8160	1.0050	0.3211	0.4400
				Weighted mode		-0.1115	0.0299	0.0004	-0.1701	-0.0528	0.8950	0.8440	0.9490	0.3211	0.4400
eqtl-a-ENSG00000132170(*PPARG*)	ieu-b-5086	Sepsis	|| id:eqtl-a-ENSG00000132170	MR Egger	212	0.0604	0.0428	0.1599	-0.0235	0.1443	1.0620	0.9770	1.1550	0.7850	0.9972
				Weighted median		0.0601	0.0304	0.0485	0.0004	0.1197	1.0620	1.0000	1.1270	0.7850	0.9972
				Inverse variance weighted (fixed effects)		0.0708	0.0197	0.0003	0.0322	0.1094	1.0730	1.0330	1.1160	0.7850	0.9972
				Simple mode		0.0383	0.0600	0.5232	-0.0792	0.1558	1.0390	0.9240	1.1690	0.7850	0.9972
				Weighted mode		0.0766	0.0318	0.0168	0.0143	0.1388	1.0800	1.0140	1.1490	0.7850	0.9972
eqtl-a-ENSG00000136810(*TXN*)	ieu-b-5086	Sepsis	|| id:eqtl-a-ENSG00000136810	MR Egger	113	-0.1116	0.0515	0.0325	-0.2125	-0.0106	0.8944	0.8085	0.9895	0.0000	0.6685
				Weighted median		-0.0099	0.0493	0.8410	-0.1064	0.0867	0.9902	0.8990	1.0905	0.0000	0.6685
				Inverse variance weighted (fixed effects)		0.0701	0.0315	0.0261	0.0083	0.1318	1.0726	1.0084	1.1409	0.0000	0.6685
				Simple mode		-0.0118	0.1081	0.9131	-0.2238	0.2001	0.9882	0.7995	1.2216	0.0000	0.6685
				Weighted mode		-0.0541	0.0433	0.2138	-0.1389	0.0307	0.9473	0.8703	1.0312	0.0000	0.6685
eqtl-a-ENSG00000142208(*AKT1*)	ieu-b-5086	Sepsis	|| id:eqtl-a-ENSG00000142208	MR Egger	98	-0.1283	0.0656	0.0535	-0.2569	0.0003	0.8796	0.7735	1.0003	0.3976	0.9917
				Weighted median		-0.0544	0.0574	0.3437	-0.1669	0.0582	0.9471	0.8463	1.0599	0.3976	0.9917
				Inverse variance weighted (fixed effects)		-0.0822	0.0369	0.0259	-0.1545	-0.0099	0.9211	0.8569	0.9902	0.3980	0.9917
				Simple mode		0.0446	0.1146	0.6981	-0.1801	0.2693	1.0456	0.8352	1.3090	0.3976	0.9917
				Weighted mode		-0.0565	0.0612	0.3587	-0.1764	0.0635	0.9451	0.8383	1.0656	0.3976	0.9917
eqtl-a-ENSG00000150768(*DLAT*)	ieu-b-5086	Sepsis	|| id:eqtl-a-ENSG00000150768	MR Egger	26	-0.1006	0.8599	0.9079	-1.7859	1.5847	0.9043	0.1676	4.8780	0.9886	0.9998
				Weighted median		-0.1572	0.1523	0.3018	-0.4559	0.1413	0.8544	0.6339	1.1517	0.9886	0.9998
				Inverse variance weighted (fixed effects)		-0.0883	0.1168	0.4495	-0.3172	0.1406	0.9154	0.7281	1.1510	0.989	0.9998
				Simple mode		-0.3198	0.2672	0.2426	-0.8434	0.2040	0.7263	0.4302	1.2262	0.9886	0.9998
				Weighted mode		-0.3238	0.2922	0.2784	-0.8965	0.2490	0.7234	0.4080	1.2827	0.9886	0.9998

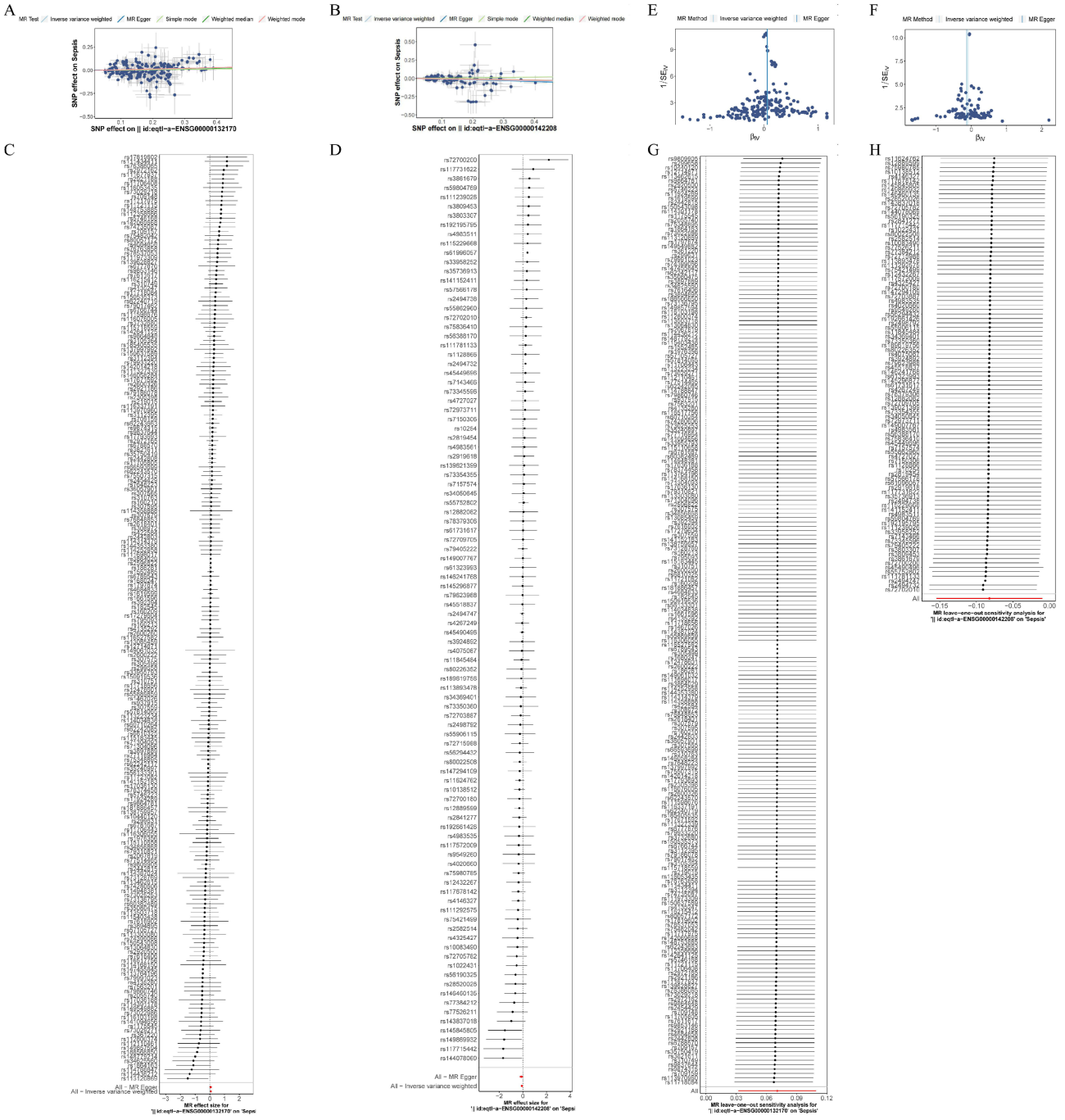

Figure 3 Mendelian randomization (MR) analysis of *PPARG*, *AKT1*, and sepsis. (**A** and **B**) Scatter plot of MR analysis results. Each point represents a single nucleotide polymorphisms (SNPs), the abscissa represents the effect size of exposure, and the ordinate represents the effect size of the outcome. (**A**) *PPARG*. (**B**) *AKT1*; (**C** and **D**) Forest plot illustrating the effect size of biomarkers on sepsis. (**C**) *PPARG*. (**D**) *AKT1*; (**E** and **F**) Funnel plots were symmetrical indicating little heterogeneity. (**E**) *PPARG*. (**F**) *AKT1*; (**G** and **H**) Leave-One-Out (LOO) analysis showing minor variations in the impact on sepsis when each SNP is sequentially excluded. (**G**) *PPARG*. (**H**) *AKT1*.

was associated with 33 pathways, including the activation of pathways such as "ribosome" "graft versus host disease" and "type I diabetes mellitus" (Figure 4B). This indicates that *PPARG* and *AKT1* play distinct roles in the development of sepsis.

To further enhance the diagnostic utility of these biomarkers, we constructed a nomogram model based on the biomarker to predict the risk of sepsis (Figure 4C). In this nomogram, individual scores for each biomarker were summed to yield an overall score that reflected the likelihood of developing sepsis, with higher scores indicating greater risk. The calibration curve of this model showed an ideal fit, with a slope close to 1, indicating high predictive reliability

https://doi.org/10.2147/JIR.S528347

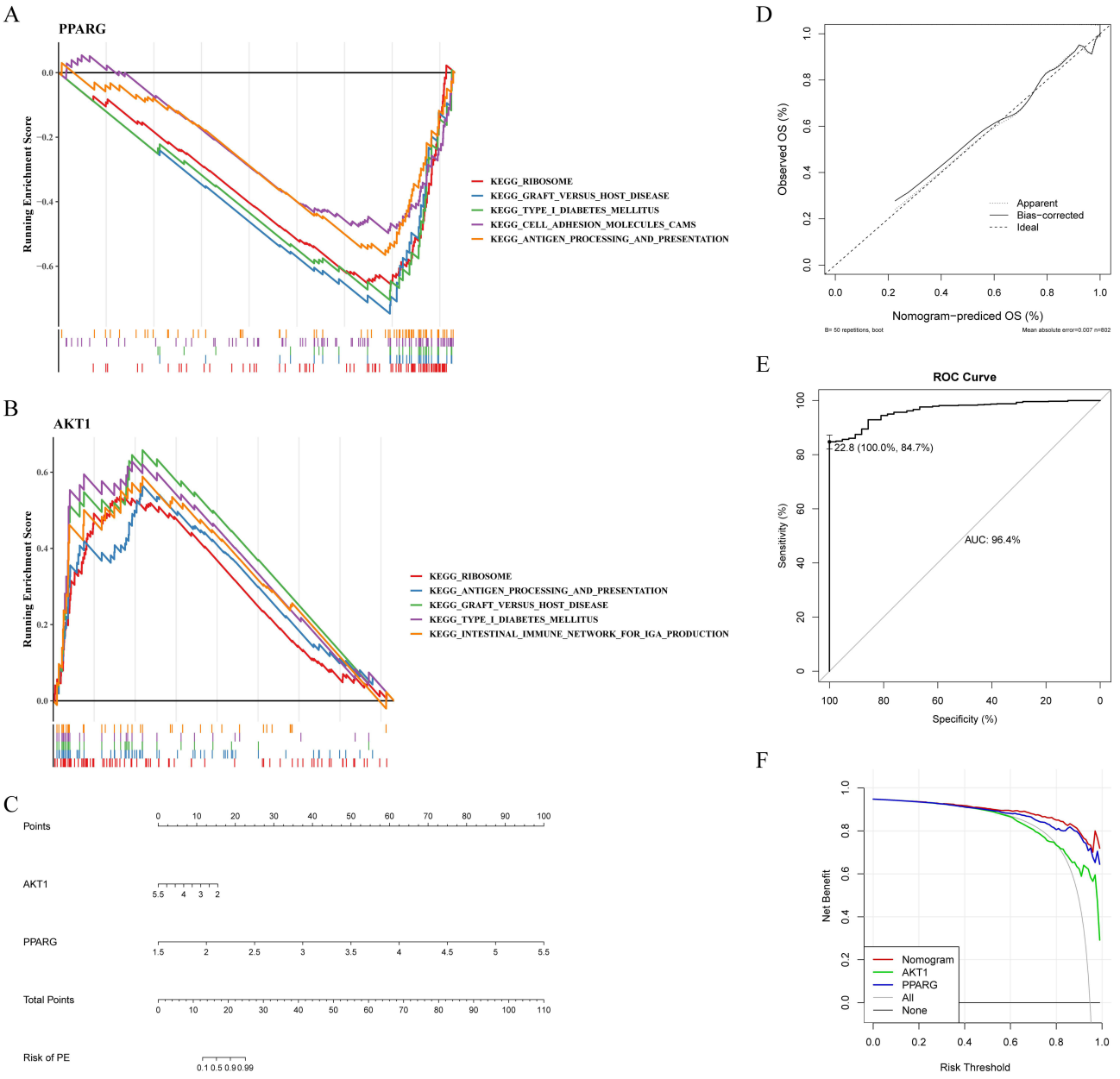

Figure 4 Function analysis and nomogram construction of *PPARG* and *AKT1*. (**A**) Gene set enrichment analysis (GSEA) of *PPARG*; (**B**) GSEA of *AKT1*; (**C**) Nomogram model based on biomarkers; (**D**) The calibration curve of the nomogram model; (**E**) The ROC curve of the nomogram model; (**F**) The decision curve analysis (DCA) of the nomogram model.

(Figure 4D). Additionally, the AUC value of the model's ROC curve was 0.964, surpassing the AUC values of *PPARG* (0.94) and *AKT1* (0.87) in the training set (Figure 4E). This confirms the strong predictive power of the combined diagnostic approach for sepsis. Finally, DCA demonstrated the clinical benefit of the model (Figure 4F).

Investigating Differences in Immune Microenvironment of Sepsis and Normal Individuals

Analysis of differences in immune cell composition between sepsis patients and healthy individuals provides insight into how the immune microenvironment influences the onset and progression of sepsis. The study illustrated the proportions of individual immune cells in sepsis and control samples from the training set using stacked bar graphs (Figure 5A). Wilcoxon test analysis revealed significant differences in the infiltration of 24 immune cell types between sepsis and control

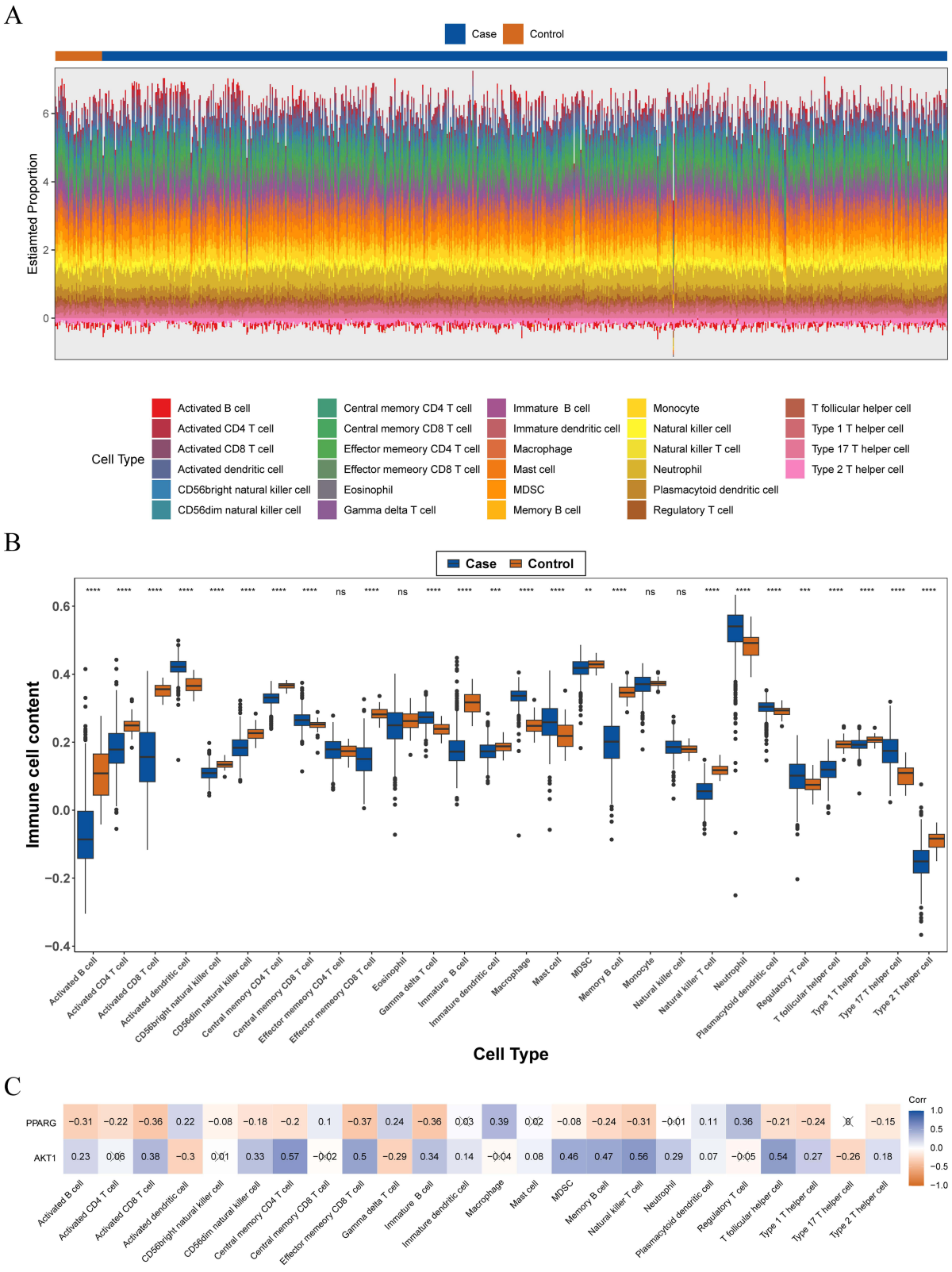

Figure 5 Immunoinfiltration analysis of sepsis. (**A**) Infiltration ratio of 28 kinds of immune cells; (**B**) Difference analysis of 28 kinds of immune cell scores between sepsis and control group. Ns means have not significant difference, ** means P < 0.01, *** means P < 0.001, **** means P < 0.0001; (**C**) Association of biomarkers with differential immune-infiltrating cells.

https://doi.org/10.2147/JIR.S528347

samples ($P < 0.05$) (Figure 5B). Specifically, sepsis samples showed reduced infiltration of immune cells such as activated B cells, type 2 T helper cells, and natural killer T cells, while infiltration of activated dendritic cells, neutrophils, and type 17 T helper cells was elevated. Further analysis indicated that *PPARG* was negatively associated with most immune cells, whereas *AKT1* showed positive associations. Notably, *AKT1* exhibited the highest positive correlation with central memory CD4 T cells (cor = 0.57, $P < 0.05$). Conversely, *PPARG* demonstrated the largest positive correlation with macrophages (cor = 0.39, $P < 0.05$) and the strongest negative correlation with effector memory CD8 T cells (cor = −0.37, $P < 0.05$) (Figure 5C). These findings suggested that septic patients experience inflammatory responses and sustained immune activation, indicating that *PPARG* might exert an opposing immune response compared to *AKT1*.

Molecular Regulatory Networks of Biomarker and Predictive Analysis of Drugs

Using public databases, we constructed TF-miRNA-mRNA networks for PPARG and *AKT1*. A total of 40 miRNAs and 8 TFs were predicted to have regulatory relationships with *AKT1*, including pairs like *TAL1-AKT1* and *HNF4A-AKT1*, which positively regulate the alleviation of septic conditions. Similarly, 64 miRNAs and 4 TFs were associated with *PPARG*, including regulatory pairs such as *CTCF-PPARG* and *E2F1-PPARG* that promoted the development of sepsis (Figure 6A). We also explored potential therapeutic agents targeting *PPARG* and *AKT1* using the DGIdb database. *AKT1* was predicted to interact with 71 drugs, while *PPARG* was associated with 125 drugs (Figure 6B). Notably, the interaction score between *AKT1* and gigantol was the highest at 1.479, while the highest interaction score for *PPARG* was with echinatin at 0.840. These interactions were selected for molecular docking (Table S5). The molecular binding energy for the *AKT1*-gigantol complex was −5.72 kcal/mol, and for the *PPARG*-echinatin complex, it was −4.79 kcal/mol, indicating strong stability of both complexes (Figures 6C and D).

Validation of the Biomarkers' Expression by qRT-PCR

To further substantiate the robustness of our results, we collected clinical samples and established a sepsis model to validate the expression levels of biomarkers using qRT-PCR. The results in sepsis model indicated that the expression levels of *PPARG* and *AKT1* were significantly reduced in the sepsis group, with the expression trend of *AKT1* aligning with bioinformatics predictions (Figure 7A). In the clinical sample verification, the expression trend of *AKT1* was found to be consistent with that observed in the mouse model, exhibiting statistically significant differences (Figure 7B). The expression trend of *PPARG* may be attributed to factors such as sample size, species differences, tissue heterogeneity, and other variables.

Discussion

The pathogenesis of sepsis is a highly intricate process, encompassing not only dysregulated host responses but also systemic disturbances in multiple organ functions.[43,44] Disturbed glucose metabolism represents a pivotal pathophysiological process in sepsis, affecting not only energy supply and cellular function but also multiple facets of the inflammatory response, immune regulation and oxidative stress.[45,46] In patients with sepsis, abnormalities of glucose metabolism manifest as insulin resistance, hyperglycaemia and impaired glucose utilisation. These changes are closely associated with the severity and prognosis of sepsis.[47–50] Identifying diagnostic and therapeutic biomarkers related to glucose metabolism in sepsis can provide valuable insights for clinical treatment strategies. Therefore, this study conducted bioinformatics research by integrating transcriptomic analysis and Mendelian randomization, successfully identifying and validating the biomarkers associated with sepsis-induced glucose metabolism disorders—*PPARG* and *AKT1*. In this study, both *AKT1* and *PPARG* demonstrated AUC values greater than 0.85 in both the training and validation sets. Notably, the AUC value for *PPARG* in the validation set reached as high as 0.98, indicating its excellent ability to differentiate between sepsis and normal samples. Their diagnostic performance is significantly superior to many commonly used biomarkers in sepsis, such as CRP ($CRP_{AUC} = 0.76$, $PCT_{AUC} = 0.72$, $IL\text{-}6_{AUC} = 0.71$, $HMGB1_{AUC} = 0.58$, $PSP_{AUC} = 0.75$).[51] This discovery not only offers potential biomarkers for the early diagnosis of sepsis but also provides new therapeutic targets for interventions targeting glucose metabolism disorders.

It has been established that in a state of septic shock, there is a tendency for dysregulation of glucose metabolism to exacerbate the inflammatory response. This may, in turn, lead to further metabolic dysfunction within the body.[52] The study of

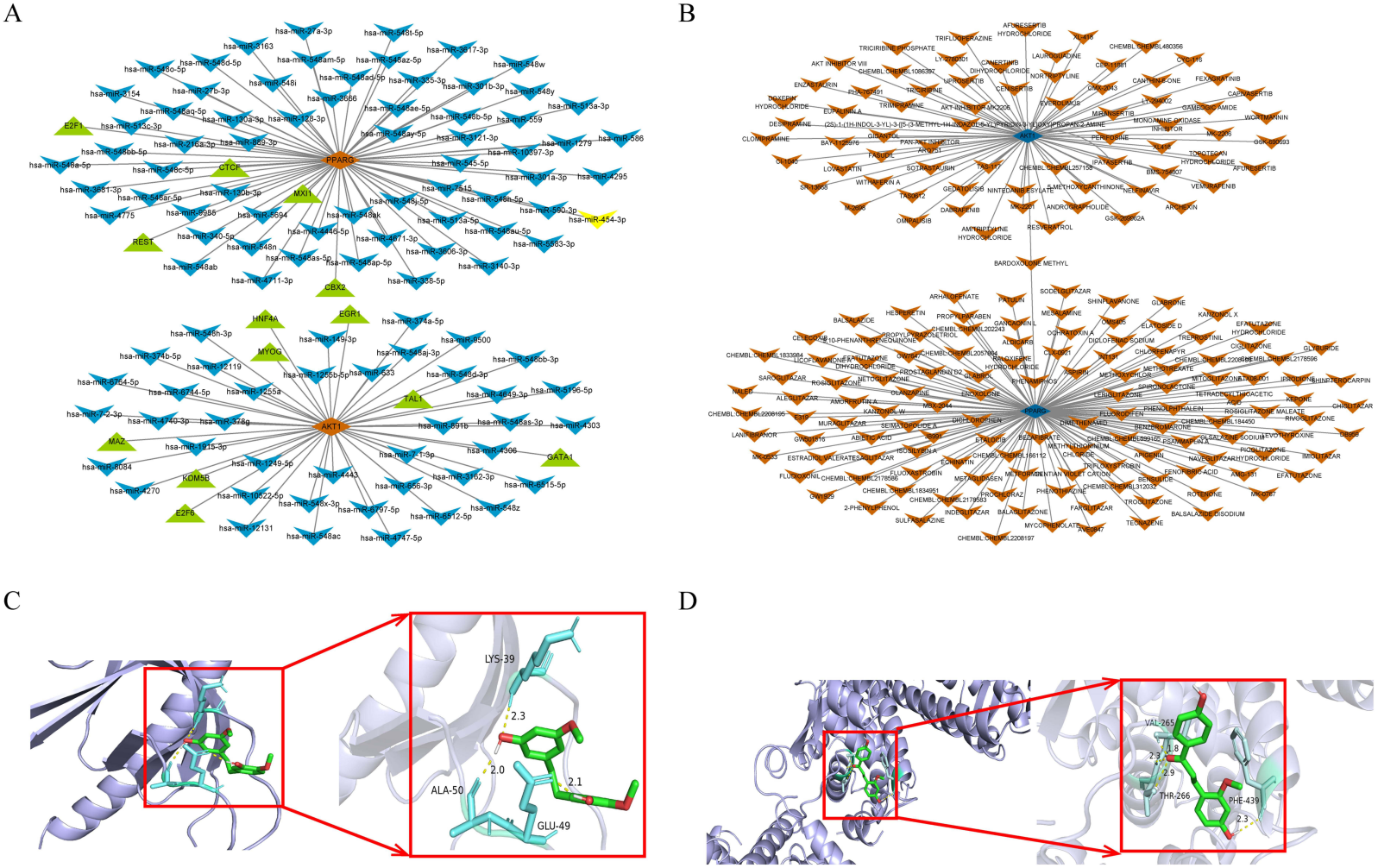

Figure 6 Molecular regulatory networks of biomarker and predictive analysis of drugs. (**A**) Construction of the molecular regulatory networks of biomarkers. Yellow indicates biomarker, blue indicates microRNAs (miRNAs), and green indicates transcription factors (TFs); (**B**) Drug prediction of biomarkers; (**C**) Molecular docking of *AKT1* to gigantol; (**D**) Molecular docking of *PPARG* to echinatin.

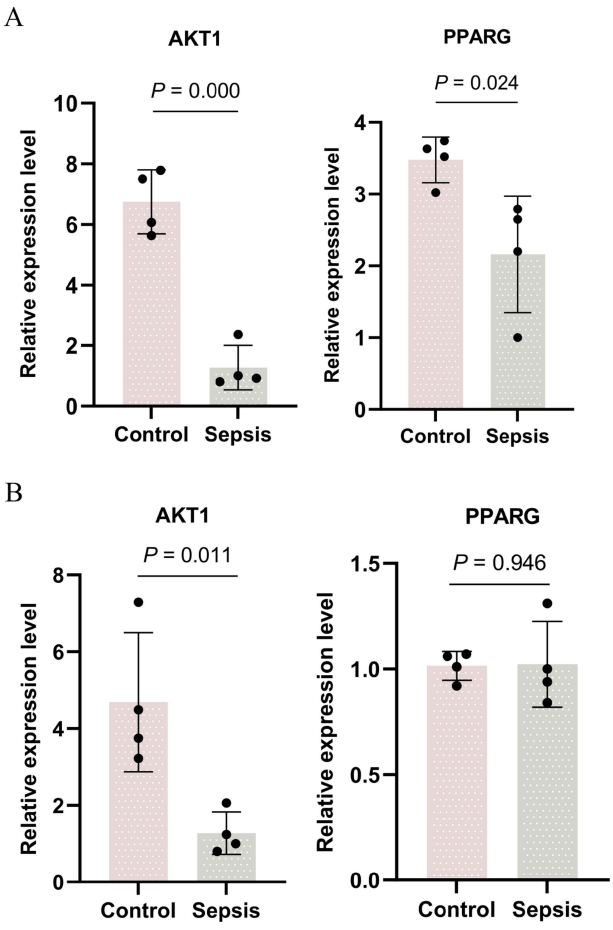

Figure 7 Validation of the biomarkers by qRT-PCR. (**A** and **B**) The results of qRT-PCR in the mouse model (**A**) and clinical samples (**B**), ($n_{Control}$ = 4, n_{Sepsis} = 4).

the role of the *PPARG* activation in the context of immune response, inflammatory processes and metabolic regulation has yielded significant findings, cell proliferation and cell differentiation.[53,54] Existing studies have demonstrated that increased expression of the *PPARG* gene has been observed to decrease levels of reactive oxygen species (ROS) and to inhibit the TXNIP/NLRP3 signalling pathway, thereby contributing to the reduction of pyroptosis and liver dysfunction during the course of sepsis.[55] In addition, upregulation of the *PPARG* gene has been shown to allow IL-37a to exert its function in immune response modulation and to inhibit inflammation through a process that does not involve the IL-1R8 receptor.[56] Notably, our findings indicate a potential association between increased risk of sepsis and the expression of the *PPARG* gene. This association may be attributable to gene polymorphisms, with the rs10865710 polymorphism of the *PPARG* gene being a particular focus of research.[57] Research has shown that the activation of *PPARG* has a protective effect against organ dysfunction caused by sepsis by regulating inflammatory pathways and reducing cell death mechanisms such as apoptosis and necrosis, particularly in the heart and liver.[58] *PPARG* has been identified as a key gene in the glycolytic pathway, which plays a central role in coordinating immune responses during sepsis. The differential expression of *PPARG* and its association with immune cell subtypes highlight the importance of its complex interactions between metabolism and immune responses under septic conditions.[59,60] The function of the *PPARG* gene is crucial in the regulation of glucose metabolism. Some studies have shown that activation of the *PPARG* gene is closely associated with improved insulin sensitivity, especially in diabetic patients, and that it can regulate glucose metabolism homeostasis in vivo and improve insulin resistance.[61] This mechanism underscores the potential of *PPARG* not only to play a pivotal role in metabolic diseases, but also to influence the prognosis of sepsis patients by regulating their metabolic status. Overall, *PPARG* exerts its protective effect in sepsis by regulating immune responses, inflammation, metabolism and cell survival mechanisms, and may affect the prognosis of sepsis by improving metabolic function.

On the other hand, the activation of the PI3K/AKT/mTOR pathway has been shown to inhibit functional cell apoptosis and reduce inflammation and oxidative stress, which in turn ameliorates sepsis-induced organ damage.[62,63] *AKT1* is a pivotal regulator of cell survival and metabolism and a signal transduction protein that performs a variety of functions within cells.[64] It has been hypothesised that the small molecule compound 7460–0250 activates the AKT-mTOR pathway, specifically promotes the phosphorylation of *AKT1* and attenuates acute lung injury in sepsis.[65] Another study has shown that puerarin, which has anti-inflammatory properties, exerts a protective effect against sepsis-associated encephalopathy by regulating the *AKT1* pathway in microglia. This regulation helps reduce neuroinflammation and cognitive impairment associated with sepsis, suggesting that targeting *AKT1* may be beneficial for managing complications related to sepsis.[66] These findings collectively suggest that enhanced expression of *AKT1* is important in the pathological development of sepsis and may serve as a key molecule in preventing sepsis progression.The role of *AKT1* in glucose metabolism is controversial. Early studies have indicated that *AKT1* knockout mice exhibit a normal metabolic profile; therefore, *AKT1* may be non-essential in the process of glucose metabolism,[67] although other studies have shown that the insulin sensitivity of mice with low blood glucose and elevated serum glucagon concentrations was improved by the absence of *AKT1*.[68] Recent studies have demonstrated that the interaction of transforming growth factor-β1 stimulated clone 22 D4 (TSC22D4) and *AKT1* promotes insulin sensitivity and regulates insulin signalling and glucose metabolism.[69] Research has shown that Wenqing Decoction can protect against sepsis-induced acute lung injury by regulating the PI3K/AKT pathway,[70] which reflects the protective role of *AKT1* in sepsis to some extent. This is consistent with our Mendelian findings. In summary, these findings highlight the multifaceted potential significance of *AKT1* in sepsis and glucose metabolism regulation, suggesting that targeting this pathway may provide new therapeutic strategies for managing sepsis-related complications.

In order to ascertain whether there is a correlation between the expression of the genes *PPARG* and *AKT1* and the specific biological pathways and functions in sepsis, GSEA was utilised to identify their potential pathways of action. The results demonstrated that both genes were associated with pathways such as ribosome, graft versus host disease, type 1 diabetes mellitus and antigen processing and presentation. Notably, enrichment analysis indicated that, in contrast to *AKT1*, the expression pattern of *PPARG* exhibited an opposite trend, suggesting a divergent role for these two genes, a hypothesis that is further substantiated by the results of this study. Ribosomes, the site of intracellular protein synthesis, have been demonstrated to play a role in cell proliferation and apoptosis.[71–74] During the state of sepsis, the body experiences heightened metabolic activity, and consequently the synthesis of significant quantities of protein is required, a process that the ribosome must facilitate. Nevertheless, if ribosomes are subjected to persistent overloading, they may incur damage, resulting in dysfunction.[75] Impaired ribosome function has been shown to induce ribosomal toxic stress, which in turn activates the MAPK signalling pathway, thereby promoting adaptive responses and restoring intracellular homeostasis.[76,77] Taurine has been shown to attenuate septic lung injury by suppressing inflammatory responses and oxidative stress through inhibition of the p38 MAPK signalling pathway.[78] P38 MAPK and MKP-1 control the glycolytic program through the bifunctional glycolytic regulator *PFKFB3* during sepsis.[79]

Graft-versus-host disease (GVHD) and sepsis share similar inflammatory and immune responses. It is well known that GVHD is a complication of stem cell or bone marrow transplantation, where transplanted cells from the donor trigger an abnormal immune inflammatory response in the recipient, leading the immune system to attack its own tissues and organs.[80] The core of sepsis pathogenesis lies in the imbalance of dynamic regulation of inflammatory responses and immune dysfunction. When pathogens invade the body, they bind to pattern recognition receptors in the innate immune system, resulting in the release of various pro-inflammatory cytokines. This leads to an overactive immune response and further culminates in a cytokine storm,[81,82] causing intense and excessive inflammatory reactions. Consequently, immune cells release large amounts of reactive oxygen species, proteases, and other cytotoxic substances, exacerbating tissue and organ damage.[83] However, as sepsis progresses, the compensatory anti-inflammatory response accompanying the initial pro-inflammatory reaction becomes overly vigorous, resulting in significant immunosuppression.[84–86]

Antigen processing and presentation constitutes a pivotal component of acquired immunity, playing a role in the recognition of pathogenic antigens. This process involves the degradation of exogenous or endogenous antigens into short peptides, which are then presented to CD4 T cells and CD8 T cells via major histocompatibility complex (MHC) molecules.[87] Antigen processing and presentation has been shown to be down-regulated in sepsis patients compared to healthy subjects, but its expression has been found to positively correlate with patient survival, suggesting a protective role for this pathway in sepsis.[88]

As mentioned earlier, during the onset of sepsis, both pro-inflammatory and anti-inflammatory processes are activated simultaneously.[89] Conducting immune-related analyses on sepsis patients to understand changes in the immune microenvironment can aid in the early diagnosis of sepsis and reflect the severity of the condition. Our correlation analysis of biomarkers with differentially infiltrating immune cells indicates that *AKT1* has the strongest positive correlation with central memory CD4 T cells, while *PPARG* shows the strongest positive correlation with macrophages. In the early stages of sepsis, macrophages, as key immune cells, are excessively activated. The *TLR4* on the surface of macrophages can recognize LPS, thereby activating inflammatory signaling pathways such as NF-κB and MAPK, leading to the release of a large number of pro-inflammatory cytokines and inducing various anti-infection mechanisms to promote inflammation and pathogen clearance.[90] As the pathophysiology of sepsis progresses, there is also a significant occurrence of apoptosis in macrophages. Meanwhile, M2-like macrophages secrete numerous anti-inflammatory mediators to suppress excessive inflammatory responses. However, with the apoptosis of various immune cells, including macrophages, T lymphocytes, and B lymphocytes, M2 phenotype macrophages can induce immunosuppression and increase the risk of infection.[91]

$CD4^+$ T cells play a crucial role in adaptive immunity by assisting Tc cells and antibody-mediated immune responses. They are activated through the recognition of MHC-II and subsequently differentiate into various effector $CD4^+$ T cell subsets,[92] such as Th1, Th2, and Th17. Th1 and Th2 are two mutually inhibitory subsets of $CD4^+$ T cells. Studies have shown that in the early stages of sepsis in mice, the level of Th1 increases, releasing pro-inflammatory cytokines that further activate macrophages and promote inflammation and pathogen clearance mechanisms. However, as sepsis progresses, the number of Th1 cells significantly decreases, leading to the differentiation of $CD4^+$ T cells into Th2 cells, which causes immunosuppression in sepsis.[93] In a normal organism, there is a dynamic balance between Treg and Th17 cells; however, in sepsis patients, the ratio of Treg to Th17 is significantly elevated, indicating a weakened ability to clear pathogens and impaired immune function.[94] We speculate that the roles of *AKT1* and *PPARG* in sepsis may be related to the quantity and function of immune cells.

The transcription factor prediction results presented here correspond with the findings of studies on the subject. The aforementioned studies identified transcription factors such as *TAL1*[95] and *HNF4A*[96] as being positively regulated by *AKT1*, which is associated with the alleviation of sepsis. Furthermore, the studies identified TFs such as *CTCF*[97] and *E2F1*[98] that are associated with the promotion of sepsis development. In the present study, a selection of drugs was identified on the basis of their strongest interactions with *AKT1* and *PPARG*. This selection was then subjected to molecular docking, with *AKT1*-gigantol and *PPARG*-echinatin proving to be the most effective. Gigantol is a benzyl compound extracted from various medicinal plants and has demonstrated potential anti-inflammatory properties in preclinical pharmacological testing systems. It effectively reduces the levels of pro-inflammatory markers and arachidonic acid metabolites through multiple pathways such as NF-κB, AKT, PI3K, and JNK/cPLA2/12-LOX.[99] Echinatin is a bioactive flavonoid derived from the licorice plant, widely used in traditional herbal medicine.[100] In vivo experiments have shown that echinatin significantly inhibits the activation of the NLRP3 inflammasome and improves LPS-induced septic shock and dextran sulfate sodium (DSS)-induced colitis in mice.[101] Besides, gigantol has been shown to alleviate inflammatory responses in the liver of mice,[102] while echinatin has been shown to intervene in sepsis by modulating NF-κB and MEK/ERK signalling pathways.[103] In summary, *AKT1* and *PPARG* are potential therapeutic drugs for sepsis, and the specific mechanism of action still needs to be further verified in the septic model.

Our study comprehensively elucidated the functional mechanisms of the glycolysis-related biomarkers *AKT1* and *PPARG* in sepsis. However, certain limitations remain in our research. Although we utilized training and validation datasets, the sample size was still relatively small, and future studies should expand the sample size to enhance the reliability of the results. The efficacy, sensitivity, specificity, and clinical performance of biomarkers need further validation in clinical samples. While we validated biomarker expression by establishing mouse model and through clinical samples, there is a need to increase the number of clinical samples for further validation. In the future, we will continue to explore the mechanisms of action of key biomarkers. These biomarkers have the potential to serve as crucial clues in future research, helping us further investigate the pathophysiological mechanisms of sepsis and providing valuable insights for clinical practice. In addition, the potential drugs targeting biomarkers obtained in drug prediction still need further experiments to explore their therapeutic effects on sepsis. In summary, this study provides a new perspective for the discovery and application of sepsis-related biomarkers, and we anticipate that it will have a positive impact on clinical practice in the future.

Conclusion

In summary, by integrating multi-omics data, bioinformatics analysis, and the MR method, we successfully identified two promising sepsis biomarkers, namely *AKT1* and *PPARG*. These findings not only provide potential targets for the early diagnosis and personalized treatment of sepsis but also lay the foundation for understanding the molecular mechanisms underlying sepsis.

Ethics Approval

This study was performed in line with the principles of the Declaration of Helsinki and approved by the Institutional Animal Care and Use Committee of the Second Clinical Medical College of Ningxia Medical University (First People's Hospital of Yinchuan) (No: KY-2025-039) and the Ethics Committee of the Second Affiliated Hospital of Ningxia Medical University (First People's Hospital of Yinchuan) (No: KY-2025-175).

Acknowledgments

Key Laboratory for Prevention and Control of Common Infectious Diseases, Ningxia Medical University has provided us with some experimental instruments.

Funding

Natural Science Foundation of Ningxia Province (Grant No. 2022AAC02061) and (Grant No. 2024AAC03787).

Disclosure

The authors report no conflicts of interest in this work.

References

1. Singer M, Deutschman CS, Seymour CW, et al. The Third International Consensus Definitions for Sepsis and Septic Shock (Sepsis-3). *JAMA*. 2016;315(8):801–810. doi:10.1001/jama.2016.0287
2. Vincent JL, Jones G, David S, Olariu E, Cadwell KK. Frequency and mortality of septic shock in Europe and North America: a systematic review and meta-analysis. *Crit Care*. 2019;23(1):196. doi:10.1186/s13054-019-2478-6
3. Chung HY, Wickel J, Brunkhorst FM, Geis C. Sepsis-Associated Encephalopathy: from Delirium to Dementia? *J Clin Med*. 2020;9(3):703. doi:10.3390/jcm9030703
4. Rudd KE, Johnson SC, Agesa KM, et al. Global, regional, and national sepsis incidence and mortality, 1990-2017: analysis for the Global Burden of Disease Study. *Lancet*. 2020;395(10219):200–211. doi:10.1016/S0140-6736(19)32989-7
5. Fleischmann-Struzek C, Schwarzkopf D, Reinhart K. Sepsis incidence in Germany and worldwide: current knowledge and limitations of research using health claims data. *Med Klin Intensivmed Notfmed*. 2022;117(4):264–268. doi:10.1007/s00063-021-00777-5
6. Xie J, Wang H, Kang Y, et al. The Epidemiology of Sepsis in Chinese ICUs: a National Cross-Sectional Survey. *Crit Care Med*. 2020;48(3):e209–e218. doi:10.1097/CCM.0000000000004155
7. McBride MA, Patil TK, Bohannon JK, Hernandez A, Sherwood ER, Patil NK. Immune Checkpoints: novel Therapeutic Targets to Attenuate Sepsis-Induced Immunosuppression. *Front Immunol*. 2020;11:624272. doi:10.3389/fimmu.2020.624272
8. Wang W, Liu CF. Sepsis heterogeneity. *World J Pediatr*. 2023;19(10):919–927. doi:10.1007/s12519-023-00689-8
9. Tindal EW, Armstead BE, Monaghan SF, Heffernan DS, Ayala A. Emerging therapeutic targets for sepsis. *Expert Opin Ther Targets*. 2021;25(3):175–189. doi:10.1080/14728222.2021.1897107
10. Pandey S. Sepsis, Management & Advances in Metabolomics. *Nanotheranostics*. 2024;8(3):270–284. doi:10.7150/ntno.94071
11. Zhang P, Pan S, Yuan S, Shang Y, Shu H. Abnormal glucose metabolism in virus associated sepsis. *Front Cell Infect Microbiol*. 2023;13:1120769. doi:10.3389/fcimb.2023.1120769
12. Collins K, Huen SC. Metabolism and Nutrition in Sepsis: in Need of a Paradigm Shift. *Nephron*. 2023;147(12):733–736. doi:10.1159/000534074
13. Wang Y, Wang X, Du C, et al. Glycolysis and beyond in glucose metabolism: exploring pulmonary fibrosis at the metabolic crossroads. *Front Endocrinol*. 2024;15:1379521. doi:10.3389/fendo.2024.1379521
14. Cheng S, Li Y, Sun X, et al. The impact of glucose metabolism on inflammatory processes in sepsis-induced acute lung injury. *Front Immunol*. 2024;15:1508985. doi:10.3389/fimmu.2024.1508985
15. Lu H, Chen Y, Yang Y, Ding M, Qiu F. lncRNA NORAD alleviates dysfunction of renal proximal tubular epithelial cells during the sepsis-associated acute kidney injury by modulating the miR-155-5p-PDK1 axis. *Environ Toxicol: Int J*. 2024;39(6):3304–3313. doi:10.1002/tox.24130
16. Tang Y, Yin L, Yuan L, Lin X, Jiang B. Nucleolin myocardial-specific knockout exacerbates glucose metabolism disorder in endotoxemia-induced myocardial injury. *PeerJ*. 2024;12:e17414. doi:10.7717/peerj.17414
17. van der Graaf A, Claringbould A, Rimbert A, et al. Mendelian randomization while jointly modeling cis genetics identifies causal relationships between gene expression and lipids. *Nat Commun*. 2020;11(1):4930. doi:10.1038/s41467-020-18716-x
18. Yu L, Liu X, Wang X, et al. Glycometabolism-related gene signature of hepatocellular carcinoma predicts prognosis and guides immunotherapy. *Front Cell Dev Biol*. 2022;10:940551. doi:10.3389/fcell.2022.940551
19. Ritchie ME, Phipson B, Wu D, et al. limma powers differential expression analyses for RNA-sequencing and microarray studies. *Nucleic Acids Res*. 2015;43(7):e47. doi:10.1093/nar/gkv007

20. Gustavsson EK, Zhang D, Reynolds RH, Garcia-Ruiz S, Ryten M. ggtranscript: an R package for the visualization and interpretation of transcript isoforms using ggplot2. *Bioinformatics*. 2022;38(15):3844–3846. doi:10.1093/bioinformatics/btac409
21. Gu Z, Hubschmann D. Make Interactive Complex Heatmaps in R. *Bioinformatics*. 2022;38(5):1460–1462. doi:10.1093/bioinformatics/btab806
22. Zheng Y, Gao W, Zhang Q, et al. Ferroptosis and Autophagy-Related Genes in the Pathogenesis of Ischemic Cardiomyopathy. *Front Cardiovasc Med*. 2022;9:906753. doi:10.3389/fcvm.2022.906753
23. Yu G, Wang LG, Han Y, He QY. clusterProfiler: an R package for comparing biological themes among gene clusters. *OMICS*. 2012;16(5):284–287. doi:10.1089/omi.2011.0118
24. Gortler J, Schulz C, Weiskopf D, Deussen O. Bubble Treemaps for Uncertainty Visualization. *IEEE Trans Vis Comput Graph*. 2018;24(1):719–728. doi:10.1109/TVCG.2017.2743959
25. Liu P, Xu H, Shi Y, Deng L, Chen X. Potential Molecular Mechanisms of Plantain in the Treatment of Gout and Hyperuricemia Based on Network Pharmacology. *Evid Based Complement Alternat Med*. 2020;2020:3023127. doi:10.1155/2020/3023127
26. Cinelli M, Sun Y, Best K, et al. Feature selection using a one dimensional naive Bayes' classifier increases the accuracy of support vector machine classification of CDR3 repertoires. *Bioinformatics*. 2017;33(7):951–955. doi:10.1093/bioinformatics/btw771
27. Li Y, Lu F, Yin Y. Applying logistic LASSO regression for the diagnosis of atypical Crohn's disease. *Sci Rep*. 2022;12(1):11340. doi:10.1038/s41598-022-15609-5
28. Yue S, Li S, Huang X, et al. Machine learning for the prediction of acute kidney injury in patients with sepsis. *J Transl Med*. 2022;20(1):215. doi:10.1186/s12967-022-03364-0
29. Sachs MC. plotROC: a Tool for Plotting ROC Curves. *J Stat Softw*. 2017;79:2. doi:10.18637/jss.v079.c02
30. Hemani G, Zheng J, Elsworth B, et al. The MR-Base platform supports systematic causal inference across the human phenome. *Elife*. 2018;7:34408. doi:10.7554/eLife.34408
31. Bowden J, Davey Smith G, Burgess S. Mendelian randomization with invalid instruments: effect estimation and bias detection through Egger regression. *Int J Epidemiol*. 2015;44(2):512–525. doi:10.1093/ije/dyv080
32. Bowden J, Davey Smith G, Haycock PC, Burgess S. Consistent Estimation in Mendelian Randomization with Some Invalid Instruments Using a Weighted Median Estimator. *Genet Epidemiol*. 2016;40(4):304–314. doi:10.1002/gepi.21965
33. Burgess S, Scott RA, Timpson NJ, Davey Smith G, Thompson SG, Consortium E-I. Using published data in Mendelian randomization: a blueprint for efficient identification of causal risk factors. *Eur J Epidemiol*. 2015;30(7):543–552. doi:10.1007/s10654-015-0011-z
34. Hartwig FP, Davey Smith G, Bowden J. Robust inference in summary data Mendelian randomization via the zero modal pleiotropy assumption. *Int J Epidemiol*. 2017;46(6):1985–1998. doi:10.1093/ije/dyx102
35. Qin Q, Zhao L, Ren A, et al. Systemic lupus erythematosus is causally associated with hypothyroidism, but not hyperthyroidism: a Mendelian randomization study. *Front Immunol*. 2023;14:1125415. doi:10.3389/fimmu.2023.1125415
36. Davey Smith G, Hemani G. Mendelian randomization: genetic anchors for causal inference in epidemiological studies. *Hum Mol Genet*. 2014;23(R1):R89–98. doi:10.1093/hmg/ddu328
37. Cui Z, Feng H, He B, He J, Tian Y. Relationship Between Serum Amino Acid Levels and Bone Mineral Density: a Mendelian Randomization Study. *Front Endocrinol*. 2021;12:763538. doi:10.3389/fendo.2021.763538
38. Hanzelmann S, Castelo R, Guinney J. GSVA: gene set variation analysis for microarray and RNA-seq data. *BMC Bioinf*. 2013;14:7. doi:10.1186/1471-2105-14-7
39. Seeliger D, de Groot BL. Ligand docking and binding site analysis with PyMOL and Autodock/Vina. *J Comput Aided Mol Des*. 2010;24(5):417–422. doi:10.1007/s10822-010-9352-6
40. Trott O, Olson AJ. AutoDock Vina: improving the speed and accuracy of docking with a new scoring function, efficient optimization, and multithreading. *J Comput Chem*. 2010;31(2):455–461. doi:10.1002/jcc.21334
41. Yan M, Chi D, Wang W, Pei P, Xie M, Li S. Characterization of Transcription Factor Krüppel-Like Factor 3 Expression in Splenic T Lymphocytes and Association with Immune Status in Septic Mice. *BIOCELL*. 2025;49:893–906. doi:10.32604/biocell.2025.063622
42. Đermić D, Ljubić S, Matulić M, et al. Reverse transcription-quantitative PCR (RT-qPCR) without the need for prior removal of DNA. *Sci Rep*. 2023;13(1):11470. doi:10.1038/s41598-023-38383-4
43. Huang M, Cai S, Su J. The Pathogenesis of Sepsis and Potential Therapeutic Targets. *Int J Mol Sci*. 2019;20(21):5376. doi:10.3390/ijms20215376
44. Giamarellos-Bourboulis EJ, Aschenbrenner AC, Bauer M, et al. The pathophysiology of sepsis and precision-medicine-based immunotherapy. *Nat Immunol*. 2024;25(1):19–28. doi:10.1038/s41590-023-01660-5
45. Kahal H, Halama A, Aburima A, et al. Effect of induced hypoglycemia on inflammation and oxidative stress in type 2 diabetes and control subjects. *Sci Rep*. 2020;10(1):4750. doi:10.1038/s41598-020-61531-z
46. Ferreira BL, Sousa MB, Leite GGF, et al. Glucose metabolism is upregulated in the mononuclear cell proteome during sepsis and supports endotoxin-tolerant cell function. *Front Immunol*. 2022;13:1051514. doi:10.3389/fimmu.2022.1051514
47. Pivonello R, Isidori AM, De Martino MC, Newell-Price J, Biller BM, Colao A. Complications of Cushing's syndrome: state of the art. *Lancet Diabetes Endocrinol*. 2016;4(7):611–629. doi:10.1016/S2213-8587(16)00086-3
48. Chao HY, Liu PH, Lin SC, et al. Association of In-Hospital Mortality and Dysglycemia in Septic Patients. *PLoS One*. 2017;12(1):e0170408. doi:10.1371/journal.pone.0170408
49. Magee F, Bailey M, Pilcher DV, Martensson J, Bellomo R. Early glycemia and mortality in critically ill septic patients: interaction with insulin-treated diabetes. *J Crit Care*. 2018;45:170–177. doi:10.1016/j.jcrc.2018.03.012
50. Rivas AM, Nugent K. Hyperglycemia, Insulin, and Insulin Resistance in Sepsis. *Am J Med Sci*. 2021;361(3):297–302. doi:10.1016/j.amjms.2020.11.007
51. He RR, Yue GL, Dong ML, Wang JQ, Cheng C. Sepsis Biomarkers: advancements and Clinical Applications-A Narrative Review. *Int J Mol Sci*. 2024;25(16):9010. doi:10.3390/ijms25169010
52. Christ A, Latz E. The Western lifestyle has lasting effects on metaflammation. *Nat Rev Immunol*. 2019;19(5):267–268. doi:10.1038/s41577-019-0156-1
53. Bougarne N, Weyers B, Desmet SJ, et al. Molecular Actions of PPARalpha in Lipid Metabolism and Inflammation. *Endocr Rev*. 2018;39(5):760–802. doi:10.1210/er.2018-00064
54. Hernandez-Quiles M, Broekema MF, Kalkhoven E. PPARgamma in Metabolism, Immunity, and Cancer: unified and Diverse Mechanisms of Action. *Front Endocrinol*. 2021;12:624112. doi:10.3389/fendo.2021.624112

55. Li Z, Liu T, Feng Y, et al. PPARgamma Alleviates Sepsis-Induced Liver Injury by Inhibiting Hepatocyte Pyroptosis via Inhibition of the ROS/TXNIP/NLRP3 Signaling Pathway. *Oxid Med Cell Longev*. 2022;2022:1269747. doi:10.1155/2022/1269747
56. Wei R, Han X, Li M, et al. The nuclear cytokine IL-37a controls lethal cytokine storms primarily via IL-1R8-independent transcriptional upregulation of PPARgamma. *Cell Mol Immunol*. 2023;20(12):1428–1444. doi:10.1038/s41423-023-01091-0
57. Lu H, Wen D, Sun J, et al. Enhancer polymorphism rs10865710 associated with traumatic sepsis is a regulator of PPARG gene expression. *Crit Care*. 2019;23(1):430. doi:10.1186/s13054-019-2707-z
58. Zhao H, Wang Y, Zhu X. Chrysophanol exerts a protective effect against sepsis-induced acute myocardial injury through modulating the microRNA-27b-3p/Peroxisomal proliferating-activated receptor gamma axis. *Bioengineered*. 2022;13(5):12673–12690. doi:10.1080/21655979.2022.2063560
59. Bian Y, Xu J, Deng X, Zhou S, Tong J. Identification of lipid metabolism-related biomarkers and prognostic analysis in geriatric patients with sepsis. *J Infect Dev Ctries*. 2024;18(10):1502–1511. doi:10.3855/jidc.19014
60. Cui D, Yu T. Unveiling the glycolysis in sepsis: integrated bioinformatics and machine learning analysis identifies crucial roles for IER3, DSC2, and PPARG in disease pathogenesis. *Medicine*. 2024;103(39):e39867. doi:10.1097/MD.0000000000039867
61. Mohammadi A, Gholamhosseinian A, Fallah H. Trigonella foenum-graecum water extract improves insulin sensitivity and stimulates PPAR and gamma gene expression in high fructose-fed insulin-resistant rats. *Adv Biomed Res*. 2016;5:54. doi:10.4103/2277-9175.178799
62. Cao YY, Wang Z, Yu T, et al. Sepsis induces muscle atrophy by inhibiting proliferation and promoting apoptosis via PLK1-AKT signalling. *J Cell Mol Med*. 2021;25(20):9724–9739. doi:10.1111/jcmm.16921
63. Li X, Wei S, Niu S, et al. Network pharmacology prediction and molecular docking-based strategy to explore the potential mechanism of Huanglian Jiedu Decoction against sepsis. *Comput Biol Med*. 2022;144:105389. doi:10.1016/j.compbiomed.2022.105389
64. Vergadi E, Ieronymaki E, Lyroni K, Vaporidi K, Tsatsanis C. Akt Signaling Pathway in Macrophage Activation and M1/M2 Polarization. *J Immunol*. 2017;198(3):1006–1014. doi:10.4049/jimmunol.1601515
65. Wang Z, Wang X, Guo Z, et al. In silico high-throughput screening system for AKT1 activators with therapeutic applications in sepsis acute lung injury. *Front Cell Infect Microbiol*. 2022;12:1050497. doi:10.3389/fcimb.2022.1050497
66. Lin SP, Zhu L, Shi H, et al. Puerarin prevents sepsis-associated encephalopathy by regulating the AKT1 pathway in microglia. *Phytomedicine*. 2023;121:155119. doi:10.1016/j.phymed.2023.155119
67. Cho H, Mu J, Kim JK, et al. Insulin resistance and a diabetes mellitus-like syndrome in mice lacking the protein kinase Akt2 (PKB beta). *Science*. 2001;292(5522):1728–1731. doi:10.1126/science.292.5522.1728
68. Buzzi F, Xu L, Zuellig RA, et al. Differential effects of protein kinase B/Akt isoforms on glucose homeostasis and islet mass. *Mol Cell Biol*. 2010;30(3):601–612. doi:10.1128/MCB.00719-09
69. Demir S, Wolff G, Wieder A, et al. TSC22D4 interacts with Akt1 to regulate glucose metabolism. *Sci Adv*. 2022;8(42):eabo5555. doi:10.1126/sciadv.abo5555
70. Xie L, Zhang G, Wu Y, et al. Protective effects of Wenqingyin on sepsis-induced acute lung injury through regulation of the receptor for advanced glycation end products pathway. *Phytomedicine*. 2024;129:155654. doi:10.1016/j.phymed.2024.155654
71. Fan Y, Cheng Y, Li Y, et al. Phosphoproteomic Analysis of Neonatal Regenerative Myocardium Revealed Important Roles of Checkpoint Kinase 1 via Activating Mammalian Target of Rapamycin C1/Ribosomal Protein S6 Kinase b-1 Pathway. *Circulation*. 2020;141(19):1554–1569. doi:10.1161/CIRCULATIONAHA.119.040747
72. Lv K, Gong C, Antony C, et al. HectD1 controls hematopoietic stem cell regeneration by coordinating ribosome assembly and protein synthesis. *Cell Stem Cell*. 2021;28(7):1275–1290e9. doi:10.1016/j.stem.2021.02.008
73. Kang J, Brajanovski N, Chan KT, Xuan J, Pearson RB, Sanij E. Ribosomal proteins and human diseases: molecular mechanisms and targeted therapy. *Signal Transduct Target Ther*. 2021;6(1):323. doi:10.1038/s41392-021-00728-8
74. Djumagulov M, Demeshkina N, Jenner L, Rozov A, Yusupov M, Yusupova G. Accuracy mechanism of eukaryotic ribosome translocation. *Nature*. 2021;600(7889):543–546. doi:10.1038/s41586-021-04131-9
75. Shao S, Hegde RS. Target Selection during Protein Quality Control. *Trends Biochem Sci*. 2016;41(2):124–137. doi:10.1016/j.tibs.2015.10.007
76. Vind AC, Snieckute G, Blasius M, et al. ZAKalpha Recognizes Stalled Ribosomes through Partially Redundant Sensor Domains. *Mol Cell*. 2020;78(4):700–713e7. doi:10.1016/j.molcel.2020.03.021
77. Vind AC, Genzor AV, Bekker-Jensen S. Ribosomal stress-surveillance: three pathways is a magic number. *Nucleic Acids Res*. 2020;48(19):10648–10661. doi:10.1093/nar/gkaa757
78. Chen J, Xue X, Cai J, Jia L, Sun B, Zhao W. Protective effect of taurine on sepsis-induced lung injury via inhibiting the p38/MAPK signaling pathway. *Mol Med Rep*. 2021;24(3):12292. doi:10.3892/mmr.2021.12292
79. Mager CE, Mormol JM, Shelton ED, et al. p38 MAPK and MKP-1 control the glycolytic program via the bifunctional glycolysis regulator PFKFB3 during sepsis. *J Biol Chem*. 2023;299(4):103043. doi:10.1016/j.jbc.2023.103043
80. Malard F, Holler E, Sandmaier BM, Huang H, Mohty M. Acute graft-versus-host disease. *Nat Rev Dis Primers*. 2023;9(1):27. doi:10.1038/s41572-023-00438-1
81. Karki R, Kanneganti TD. The 'cytokine storm': molecular mechanisms and therapeutic prospects. *Trends Immunol*. 2021;42(8):681–705. doi:10.1016/j.it.2021.06.001
82. Kargaltseva NM, Borisova OY, Mironov AY, Kocherovets VI, Pimenova AS, Gadua NT. Bloodstream infection in hospital therapeutic patients. *Klin Lab Diagn*. 2022;67(6):355–361. doi:10.51620/0869-2084-2022-67-6-355-361
83. McDonald B, Davis RP, Kim S-J, et al. Platelets and neutrophil extracellular traps collaborate to promote intravascular coagulation during sepsis in mice. *Blood*. 2017;129(10):1357–1367.
84. Torres LK, Pickkers P, van der Poll T. Sepsis-Induced Immunosuppression. *Annu Rev Physiol*. 2022;84:157–181. doi:10.1146/annurev-physiol-061121-040214
85. Liu D, Huang SY, Sun JH, et al. Sepsis-induced immunosuppression: mechanisms, diagnosis and current treatment options. *Mil Med Res*. 2022;9(1):56. doi:10.1186/s40779-022-00422-y
86. Cavaillon JM. During Sepsis and COVID-19, the Pro-Inflammatory and Anti-Inflammatory Responses Are Concomitant. *Clin Rev Allergy Immunol*. 2023;65(2):183–187. doi:10.1007/s12016-023-08965-1
87. Pishesha N, Harmand TJ, Ploegh HL. A guide to antigen processing and presentation. *Nat Rev Immunol*. 2022;22(12):751–764. doi:10.1038/s41577-022-00707-2

88. Li Q, Sun M, Zhou Q, Li Y, Xu J, Fan H. Integrated analysis of multi-omics data reveals T cell exhaustion in sepsis. *Front Immunol*. 2023;14:1110070. doi:10.3389/fimmu.2023.1110070
89. Cao M, Wang G, Xie J. Immune dysregulation in sepsis: experiences, lessons and perspectives. *Cell Death Discov*. 2023;9(1):465. doi:10.1038/s41420-023-01766-7
90. Chen X, Liu Y, Gao Y, Shou S, Chai Y. The roles of macrophage polarization in the host immune response to sepsis. *Int Immunopharmacol*. 2021;96:107791. doi:10.1016/j.intimp.2021.107791
91. van der Poll T, Shankar-Hari M, Wiersinga WJ. The immunology of sepsis. *Immunity*. 2021;54(11):2450–2464. doi:10.1016/j.immuni.2021.10.012
92. Bai G, Cui N, Wang H, et al. T-lymphocyte subtyping: an early warning and a potential prognostic indicator of active cytomegalovirus infection in patients with sepsis. *Immunol Cell Biol*. 2022;100(10):777–790. doi:10.1111/imcb.12586
93. Zhao GJ, Yang XY, Zhang C, et al. Supplementation with Nicotinamide Riboside Attenuates T Cell Exhaustion and Improves Survival in Sepsis. *Shock*. 2023;60(2):238–247. doi:10.1097/SHK.0000000000002153
94. Zhou X, Yao J, Lin J, Liu J, Dong L, Duan M. Th17/Regulatory T-Cell Imbalance and Acute Kidney Injury in Patients with Sepsis. *J Clin Med*. 2022;11(14):4027. doi:10.3390/jcm11144027
95. Noyes HA, Alimohammadian MH, Agaba M, et al. Mechanisms controlling anaemia in Trypanosoma congolense infected mice. *PLoS One*. 2009;4(4):e5170. doi:10.1371/journal.pone.0005170
96. Ehle C, Iyer-Bierhoff A, Wu Y, et al. Downregulation of HNF4A enables transcriptomic reprogramming during the hepatic acute-phase response. *Commun Biol*. 2024;7(1):589. doi:10.1038/s42003-024-06288-1
97. Siegler BH, Thon JN, Altvater M, et al. Abdominal surgery induces long-lasting changes in expression and binding of CTCF with impact on Major Histocompatibility Complex II transcription in circulating human monocytes. *PLoS One*. 2023;18(10):e0293347. doi:10.1371/journal.pone.0293347
98. Warg LA, Oakes JL, Burton R, et al. The role of the E2F1 transcription factor in the innate immune response to systemic LPS. *Am J Physiol Lung Cell Mol Physiol*. 2012;303(5):L391–L400. doi:10.1152/ajplung.00369.2011
99. Chowdhury R, Bhuia S, Rakib AI, et al. Gigantol, a promising natural drug for inflammation: a literature review and computational based study. *Nat Prod Res*. 2025;39(5):1241–1257. doi:10.1080/14786419.2024.2340042
100. Honda H, Nagai Y, Matsunaga T, et al. Isoliquiritigenin is a potent inhibitor of NLRP3 inflammasome activation and diet-induced adipose tissue inflammation. *J Leukoc Biol*. 2014;96(6):1087–1100. doi:10.1189/jlb.3A0114-005RR
101. Xu G, Fu S, Zhan X, et al. Echinatin effectively protects against NLRP3 inflammasome–driven diseases by targeting HSP90. *JCI Insight*. 2021;6(2):134601. doi:10.1172/jci.insight.134601
102. Xue Y-R, Yao S, Liu Q, et al. Dihydro-stilbene gigantol relieves CCl4-induced hepatic oxidative stress and inflammation in mice via inhibiting C5b-9 formation in the liver. *Acta Pharmacol Sin*. 2020;41(11):1433–1445. doi:10.1038/s41401-020-0406-6
103. Duan M, Jie J, Li C, et al. Echinatin alleviates sepsis severity through modulation of the NF-κB and MEK/ERK signaling pathways. *Biomed Pharmacother*. 2024;179:117359. doi:10.1016/j.biopha.2024.117359